Start modelling for heavy trucks

Master's thesis
performed in **Vehicular Systems**

by
Fredrik Mellblom

Reg nr: LiTH-ISY-EX-3560-2004

1st October 2004

Start modelling for heavy trucks

Master's thesis

performed in **Vehicular Systems**,
Dept. of Electrical Engineering
at **Linköpings universitet**

Performed for **Scania CV AB**

by **Fredrik Mellblom**

Reg nr: LiTH-ISY-EX-3560-2004

Supervisor: **Johan Lindström**
Scania CV AB
Anders Fröberg
Linköpings Universitet

Examiner: **Professor Lars Nielsen**
Linköpings Universitet

Södertälje, 1st October 2004

Titel	Startmodellering för tunga lastbilar
Title	Start modelling for heavy trucks
Författare	Fredrik Mellblom
Author	

Sammanfattning
Abstract

Modern heavy trucks tend to get more and more equipment demanding electric power. As a result, the electric power left for starting become more and more limited. If a complete view of the entire starting system — battery, starter and the combustion engine — is used, the total system can be investigated and optimized. This thesis is a study of the starting system and its components. Theories for each component are presented and models are derived for a complete starting system. Focus lies on the battery and starter motor. The purpose of the modelling work is to gain knowledge of the starting system. Some results can also be obtained from the simulations — it is very important to keep the electrical resistance as low as possible and the differences between battery types are surprisingly big.

Abstract

Modern heavy trucks tend to get more and more equipment demanding electric power. As a result, the electric power left for starting become more and more limited. If a complete view of the entire starting system — battery, starter and the combustion engine — is used, the total system can be investigated and optimized. This thesis is a study of the starting system and its components. Theories for each component are presented and models are derived for a complete starting system. Focus lies on the battery and starter motor. The purpose of the modelling work is to gain knowledge of the starting system. Some results can also be obtained from the simulations — it is very important to keep the electrical resistance as low as possible and the differences between battery types are surprisingly big.

Keywords: start modelling, cranking, lead-acid battery, starter motor

Acknowledgements

First of all I would like to thank my supervisors Johan Lindström, Anders Fröberg and my examiner Lars Nielsen. Special thanks to Niklas Pettersson for discussions and help with models. I would like to thank Michael Blackenfelt, Björn Malmgren, Kristian Lindqvist, Christer Östergård, Dan Magnusson, Daniel Bjurefors, Bengt Blomberg, Vilmos Perlaki, Seppo Kauppi, Lars-Åke Dahlqvist, Bengt Larsson, Marcus Segerstedt, Brian Trainor and Johan Lundqvist for their invaluable assistance. Also thanks to all the other people at Scania Technical Centre who have contributed to making this thesis possible.

Södertälje, Sweden   Fredrik Mellblom
September, 2004

Contents

Chapter 1

Introduction

Starting systems for heavy trucks are gaining interest due to the increase of electric load in the vehicle. This thesis is a study of starting systems for heavy trucks. The work is for everyone with interest in starting systems for heavy trucks. Foremost, the purpose is to increase the knowledge of starting system with focus on the batteries and the starter motor. To gain knowledge theories have been studied and a number of tests and simulations of starting systems have been performed. Many conclusions have been drawn from the studies. However, much work remains to be done and future work is suggested in the thesis. The work has been done at Scania CV AB, RESC, Scania Technical Centre, Södertälje.

1.1 Background and thesis motivation

Internal combustion engines must be started by a separate system. They can not start by themselves like for example electric motors. When starting internal combustion engines considerable torque has to be produced to overcome resistance from compression and friction. The torque is produced by an electric motor, called starter, and the energy for the process is taken from a battery.

Long-haulage heavy trucks more and more take the form of a limited portable home. They are equipped with TV, refrigerator and other comfort systems the driver wants. All this equipment consumes energy and several appliances are also used at standstill. They demand battery capacity and limit the energy left for starting. As a result it is more and more important to decrease the needed power to start and to be able to predict the necessary power. The traditional way to specify a starting system is focused on the mechanical properties and worst-case scenarios. When the total power and energy consumption is in focus a more complete view of the entire starting system is needed; battery, starter and the combustion engine.

1.2   Thesis objective

The goal of the work is to gain knowledge of the starting system with focus on the starter motor and the batteries. The goal of the thesis is to document the achieved knowledge and give suggestions for future work.

1.3   Methodology

The main methodology is to derive models of the starting system and thereby gain knowledge. The work started with studies of existing literature and models for starting systems. At the same time interviews were conducted with personnel at STC (Scania Technical Centre) and a study of internal reports related to starting. Existing models available at STC were also studied, with their background physics and data. Thereafter tests of complete starting systems and parts of the systems were performed to investigate the processes and characteristics of each component. The tests were repeated as the models were calibrated and simulations gave rise to new questions. Possible differences between model and test result have been looked upon and are discussed in this thesis. Models of starting systems with different components have been built, simulated and investigated.

1.4   Thesis overview

This first chapter introduces the background and goal of the thesis. The chosen simulation environment of the thesis is described in the Dymola overview.

Chapters 2, 3, 4 and 5 introduce different parts of the starting system and begin with introduction and basic theory of the component. Thereafter a few papers are mentioned and some discussion around them. In the next section the model for this work is described with limitations and features. After the model description, tests used to validate and calibrate the model and data used to make the model are described and discussed. Finally a few suggestions for future work are presented. Each chapter is written so it is possible to read separately if the reader has only interest in that part.

Chapter 6 is composed of simulations of complete starting systems with comments.

In the appendix A a detailed discussion of the tests in the engine cell can be found and a few lines may be read about starter motor tests.

1.5   Dymola overview

Dymola is a computer program made by Dynasim. In Dymola models are written in the language Modelica. Modelica is a language designed for object-oriented physical modeling. The object-orientation makes it possible to create

basic models and then for more advanced models to inherit the basic characteristics. This makes it, for example, easy to change the basic properties of all models based on the same basic model. In Modelica equations can be written in the same order as they generally appears for models derived from physical equations. There is no need to assign input and output variables and form the equations in the appropriate form. This makes the models easy to read and removes a hard and error-prone process. It also makes the models highly flexible and reusable.

Dymola is a help while writing in the Modelica language. Some model building can be done graphically and color coding, syntax check and so on are always useful. Dymola is also a compiler and produces self-executable files for the simulation with default files for simulation data. The executable file can be executed from within Dymola and the simulation results can also be viewed. Another program, like Matlab, has to be used for more advanced analyzes of the results.

A start for more information of the Modelica language is the internet site `www.modelica.org`. To find out more about Dymola and Dynasim look at `www.dynasim.com`.

Chapter 2

Battery

2.1 Overview

Lead-acid batteries are the dominant electrical energy storage for heavy trucks. In this chapter the focus is on the lead-acid battery. The lead-acid battery will be shortly described and some basic functions are discussed. Related work is presented with a number of different models. Thereafter, the battery model for this thesis described. Finally tests, simulations, results and suggestions for future work is presented.

2.2 Introduction

A vehicle needs energy to start its engine and the function to store energy is assigned to the battery. Today the flooded lead-acid battery totally dominates the market for batteries in heavy trucks. Other types of batteries are possible to use, but only flooded lead-acid batteries will be discussed in this thesis. The batteries will also only be used for discharge.

In [18] several distinct advantages are given for lead-acid batteries in vehicle duties (selected):

- The ability to deliver the very large currents required for vehicle starting in a reliable manner.

- The availability of low cost materials and cheap fabrication gives a low price.

- The system behaves well with simple voltage-limited charging system and gives a good service life.

- The chemical stability of the components over a convenient range of operating temperatures.

- The existence of recycling infrastructure.

Most heavy trucks use a 24 V system and carries two 12 V batteries. The three most used capacities for Scania trucks are 140 Ah, 175 Ah, 220 Ah. The value is assigned from a standard, C20, for battery capacity (see chapter 5.2 in [18]). The default capacity is 175 Ah, but in warmer countries 140 Ah is common and in colder countries many buyers choose the 220 Ah battery. This is because the batteries' internal resistance increases with lower temperature.

2.3   Theory

A 12 V flooded lead-acid battery is composed of six identical cells connected in series. The cells are composed of three active components; positive plate, negative plate and an electrolyte. The plates are immersed in the electrolyte. The positive plate contains lead oxide (PbO_2), the negative plate spongy lead (Pb) and the electrolyte is dilute sulphuric acid (H_2SO_4). The sulphuric acid is dissociated into negative sulphate ions (SO_4^{2-}) and positive hydrogen ions (H^+). For a schematic figure of a lead-acid cell see figure 2.1.
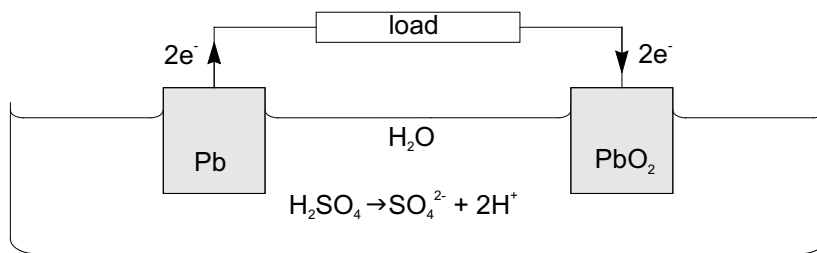
Figure 2.1: Lead-acid cell

During discharge the following reactions take place:

At the negative plate: $Pb + SO_4^{2-} \rightarrow PbSO_4 + 2e^-$

At the positive plate: $PbO_2 + H_2SO_4 + 2H^+ + 2e^- \rightarrow PbSO_4 + 2H_2O$
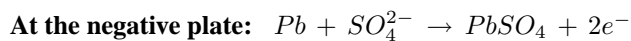
The capacity of the battery depends on the area and thickness of the plates in the electrolyte. To maximize the surface the plates are highly porous. When no current flows through the battery (and it has had some rest time) the battery is in equilibrium and an open-circuit voltage value is stable over the terminals (excluding self-discharge). When current starts to flow the voltage differs from the open-circuit value and the changes are know as polarization. In [18] three commonly known polarizations are listed:

Active polarization: Representing the energy to overcome the reaction's activation energy barriers.

Concentration polarization: Representing the changes in electrode potentials due to changes in local concentration as the reaction proceeds.

Ohmic or Resistance polarization: Representing the resistive losses in the current path through the battery components.

In a cranking process the current drawn from the battery is very high. At these high currents very complex phenomena occur inside the battery. One likely limit is the acid inside the porous plates. The reaction goes faster than the transport of new acid ions in the electrolyte. Thus is the acid concentration becomes locally low inside the plates and this limits the power delivered from the battery.

State of charge is an important concept in battery theory. A battery is seldom at its full capacity and therefore it is important to know the amount of charge left. A battery's state of charge is usually defined as the charge available from the battery, expressed as a fraction of rated capacity. Further information on state of charge can be found in chapter 5.7 in [18].

For further studies of batteries the book [18] is recommended.

2.4 Related work

A battery has very complex physical characteristics. It is hard to design a single model that describes batteries accurately in different applications. You have to decide exactly what environment your model should describe and build a model based on that fact.

A battery is a chemical device. Therefore it would seem that a chemical model would be the best. A chemical model based on cell characteristics such as electric potential, electrolyte concentration, diffusion, active surface area, exchange current density, and so on; for example a thermodynamical model. The model can with good approximation be one dimensional as showed in the papers [9] and [3].

When the battery is an energy supplier it is easier to view the battery as a black box and assign electrical properties, such as resistance and capacitance, to the model.

The simplest model is just a fixed-voltage source in series with a resistance. This model is for example used in [15] and may work fine if you do not need to capture the dynamic behaviour more accurately.

The next step is a Thevenin battery model, see figure 2.2. The model consists of a fixed-voltage source in series with a resistance and an RC-link. This model is widely known and used. It is also often used as a base for more complex models. In [2] a Thevenin model is used as a short-term discharge model, up to five seconds. The second model in this paper is also based on a Thevenin model and introduces more long-term effects as self-discharge and gaseous processes.
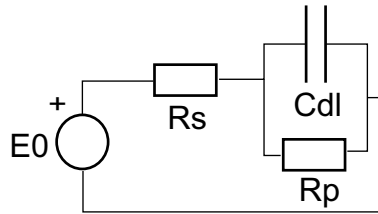
Figure 2.2: Thevenin battery model.

The Thevenin model can for example be modified in the following ways:

- replace fixed-voltage source with a capacitor to model battery capacity

- introduce self-discharge resistance to describe the self-discharge of the battery

- introduce diodes so different resistances are used for charge and discharge of the battery

- add more RC-links to better model different time constants

If you replace the capacitor in the RC-links with constant phase elements, you get ZARC-elements instead of RC-links. This approach might yield better results in some applications and is for example discussed in [21].

A different electric model was invented by C.M. Sheperd and is described in [19]. The model is for example used in the paper [4]. Shepherd's model:

$$V_b = V_{oc} - (R_b + K \frac{q_0}{q_0 - q})I_a$$

V_b: battery terminal voltage

V_{oc}: battery open-circuit voltage in volts

q_0: battery capacity in ampere-hours

R_b: battery ohmic resistance in ohms

K: polarization resistance in ohms

I_a: discharge current in amperes

$q = \int_0^t I_a dt$: accumulated discharge in ampere-hours

The model is based on constant currents, so you have to be very careful and stay close to the current the model is calibrated for.

2.5 Model

There are many proposals for battery models. The battery model chosen for this thesis has some unusual features and limitations. Many other models handle both charging and discharging. In this thesis only discharge is present. The interesting discharge rate is extremely high, from around 200 A to 2000 A, but due to the available test equipment the model is only calibrated for currents up to 1000 A. Only the voltage over the battery during discharge is of interest, how the voltage rises after discharge does not affect the starter and thereby not the starting system. The simulation time is short, up to 20 seconds, and this is the time duration of the model. The state of charge, how much energy the battery has left, is an important variable in any battery model. Due to the time available for tests the state of charge is not a parameter in the model — all batteries are fully charged. The time limitation also resulted in tests at only two temperatures; -18°C and $+20^\circ$C. Any heating is neglected since the time of simulation is so short that the energy due to losses in the battery is small compared to the battery heat capacity.

To summarize, the model characteristics:

- Only discharge.

- High current, 200 A to 1000 A.

- Short time, up to 20 seconds.

- No self-discharge (too short time).

- Only batteries with high state of charge.

- Only calibrated at two temperatures; -18°C and $+20^\circ$C.

- No heating.

With this focus many different battery models were tried, for example based on the three polarization effects (see chapter 2.3) and the models suggested in related papers. The model should both describe the wanted characteristics and be compatible with the tests possible to perform. Finally an enhanced version of the Thevenin battery model was developed. The most important modification is the resistance; which is divided into a constant resistance and a current dependent resistance. There is also a voltage loss component introduced, which models the voltage drop as the battery is discharged. In figure 2.3 the Dymola model can be viewed.

2.5.1 Interfaces

The model has two interfaces; the electrical plus and minus terminals of the battery. There is no electrical ground placed inside the battery model.
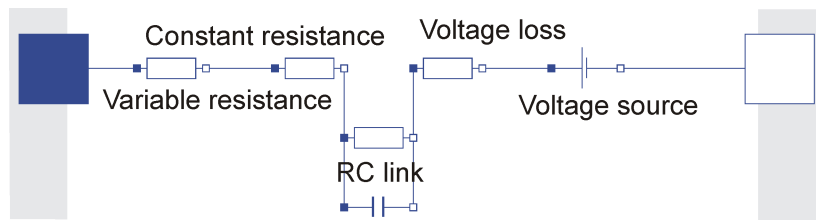
Figure 2.3: Battery model from Dymola.

2.5.2   Voltage source

The voltage source is a fixed-voltage source with the initial open-circuit voltage value. The drop of virtual open-circuit voltage due to discharge is modelled in the voltage loss component.

The voltage source component depends only on its initial value.

2.5.3   Voltage loss

Voltage drop due to discharge is modelled as a drop of voltage over a component called voltage loss. The voltage drop is calculated as a constant value, depending on battery capacity, multiplied with the sum of current taken from the battery. The modelled voltage loss is independent of the instantaneous current, but this is an approximation (see chapter 2.7). The model is best fitted for currents from 300 A to 600 A at $+20°$C and 600 A to 1000 A at $-18°$C.

The voltage loss depends on battery capacity, temperature and total current taken from the battery.

2.5.4   Variable resistance

The tests resulted in a resistance depending on the instantaneous current delivered by the battery. The resistance drops with higher current. Its maximum is at 100 A; if the current drops lower the resistance is kept at the value for 100 A. The minimum resistance is at 1000 A. The resistance for this component drops to zero at 1000 A (and newer goes below zero). For higher currents the resistance is constant and is modelled in the constant resistance. The resistance as a function of current can be seen in figure 2.6.

The variable resistance depends on battery capacity, temperature and current.

2.5.5   Constant resistance

The lowest resistance value from the tests was found at the maximum current, 1000 A. This resistance is modelled in the constant resistance component.

The value depends only on battery capacity and temperature.

2.5.6   RC-link

The transient behaviour of the battery is modelled as an RC-link. This is directly inherited from the basic Thevenin model. More RC-links and other components describing the behaviour of the battery could be added for further resemblance between the model and test results. This is further discussed in chapter 2.4 and 2.6.

The values depend on battery capacity and temperature.

2.5.7   Battery box

Most heavy trucks use a 24 V system. In these trucks a battery is never alone; two batteries are always connected in series. Therefore a component has been created which holds two batteries. Figure 2.4 shows the model. The battery box model has a default open-circuit voltage of 26 V. The component also contains the electric ground of the simulation.
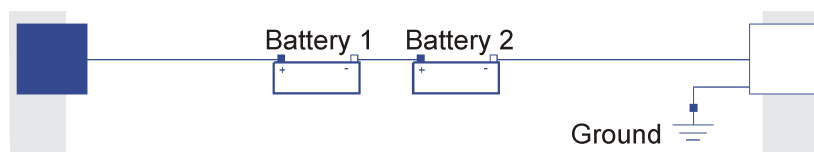
Figure 2.4: Battery box model from Dymola.

2.6   Tests

Tests have been done in the battery laboratory at STC. No effort was made to measure internal battery values like; acid weight or local potentials. All preparations and tests have been done at room temperature. When characteristics at $-18°$C were investigated the batteries were cooled after charge.

The batteries were charged with the laboratory equipment until the charge current had been reduced to a few amperes. The batteries were thereby at a high state of charge. One battery at a time was thereafter connected to a current limiting equipment, Digatron HEW 1000. At the minus side a shunt was connected for current measurement. Voltage and current was recorded with a RoadRunner modulo 1 (the RoadRunner was also used for other tests and is described more in appendix A). The HEW is able to control currents up to 1000 A. Three different tests were tried:

- step-response: 600 A for fifteen seconds.

- step-response: 1000 A for fifteen seconds.

- stair-function: started with 1000 A and then steps of one hundred amperes down to 100 A and then back again for eighteen seconds.

The step-responses were hard to use for model building. The results were highly individual and any model parameters hard to determine. The data was not used. The results were although interesting and gave some basic battery understanding and information for very high currents. The two most interesting results were that the total polarization depends on the current and that the voltage falls with current output.

The stair-function gave more steady results, but had some interesting limitations. The HEW is only possible to control manually. Discharge current is set by turning a wheel at the front of the machine. As a result the stair-function depends on the operator. This is not really a problem since another characteristic of the HEW limits the transient functionality of the equipment. The HEW is built for a constant current. Every time the current changes a peak of 1000 A for around two milliseconds appears. This limiting factor highly diminishes the test equipment's value for transient measurements. For any more advanced measurements outside parties must be contracted. Despite these limits the stair-function was found to offer results for model building. The constant parts of the steps could be used to calculate polarization for different currents. The increasing polarization could be used to get a rough estimation of the voltage drop over delivered current. The transient behaviour could be used to get rough values for the RC-link of the model.

Only the stair-function was repeated with cooled batteries, and only using batteries of the capacities 175 Ah and 220 Ah. This was due to limits of time and access to equipment. The batteries were charged at room temperature and thereafter cooled.

Why the resistance drops with higher current is not discussed in this thesis. The phenomenon may probably be found in the complex behaviour of the battery chemistry.

The measurements were often noisy and the most prominent source for this was the HEW. No investigation how the HEW is built has been performed, but it is suspected that the feedback control introduces noise and that there is overhearing from the internal AC voltage parts.

2.7   Simulation and model calibration

Simulations of a stand-alone battery were mostly done in Matlab. The Matlab model was then directly transferred to Dymola.

The procedure to find parameter values were like follows:

1. Adjust collected test data with calibration values for the equipment.

2. Plot the data as polarization (voltage over current) for each hundred ampere (see figure 2.5).

3. Find voltage loss value such that the polarization, now seen as resistance, becomes independent of time.

4. Calculate mean values of resistance for each hundred ampere (see figure 2.6).

5. Find RC-link values such that the simulated voltage follows the measured voltage.

The voltage drop is not constant for the instantaneous current. Higher currents give a higher value for the constant. This effect is more obvious at lower temperatures and for lower capacity batteries. The effect is not modelled since it is small and the current is most of the time between 300 A and 600 A at $+20°$C and 600 A to 1000 A at $-18°$C.

The resistance was found to be dependent of the current. There is a very small dependence of the direction of the stair, but it was clearly possible to neglect.

In figure 2.5 the polarisation of a 175 Ah battery at $-18°$C can be viewed. Things to note in the figure:

- The polarisation decreases with increased current.

- The polarisation increases with time (or sample number in figure).

In figure 2.6 the resistance for different batteries at different temperatures can be viewed. Things to note in the figure:

- The resistance decreases with increased current.

- Batteries with greater capacity have lower resistance.

- Temperature has a dominant effect on the resistance and lower temperature increases the resistance.

The values of the RC-link were found by plotting and adjusting the values so the simulated voltage followed the measured voltage. This was done by hand since it was found to be easiest. The values are very rough due to the limitations in the test (discussed in chapter 2.6).

In figure 2.7 the measured and simulated voltage over a 175 Ah battery at $+20°$C is shown. The test procedure is as described in chapter 2.6. The high initial drop of voltage could be better modelled if an additional RC-link is added to the model, but it is not significant for the complete system simulation at its present complexity. Only the first 10 s are shown, the model is optimized for 20 s.

Since the resistance drops with increased current, it is possible that the losses in the battery would be lower for a higher current. The power loss in diffrent batteries are shown in figure 2.8 and it does increase with current, lower temperature and lesser battery capacity.

2.8   Future work

Due to limits in time for tests and limits in the available test equipment much
work can be done to develop a better battery model. A few suggestions are
mentioned here:

- Only measure batteries known to be in the middle of their lifetime or
  introduce a parameter for battery age.

- Wider state of charge range. Batteries normally operate at a state of
  charge in between 30-70%.

- Introduce model components and do more tests to improve model tran-
  sient behaviour.

- If the initial peak of a starting system simulation shall be reliably sim-
  ulated the battery model must be increased to higher currents and im-
  prove transient functionality.

- If a more complete investigation of the inner processes of the battery is
  needed, a battery model based on thermodynamics or collision theory
  could be used.
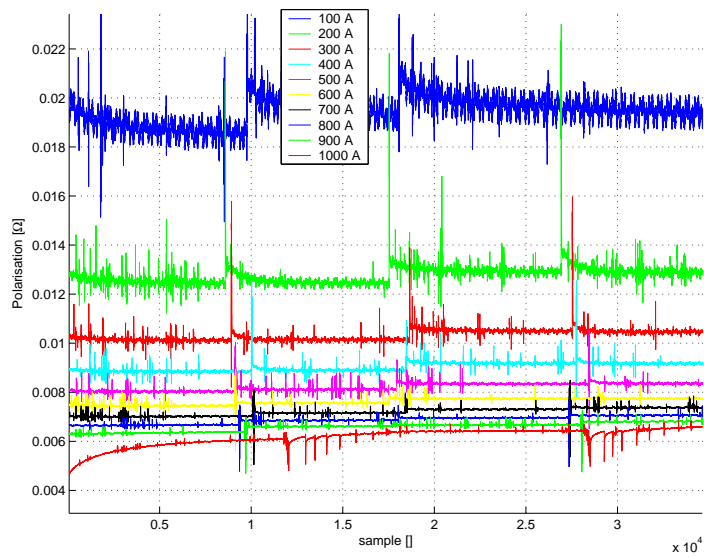
Figure 2.5: Battery polarisation for different currents. Test with 175 Ah battery at $-18°$C.
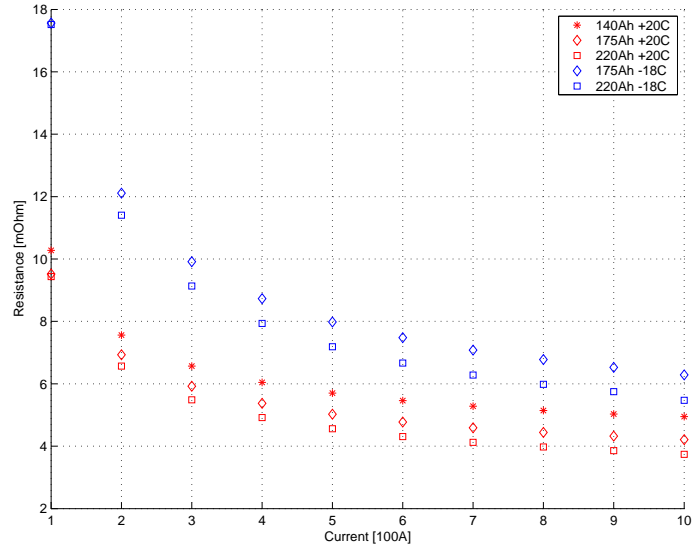
Figure 2.6: Resistance as a function of current for different batteries and temperatures.
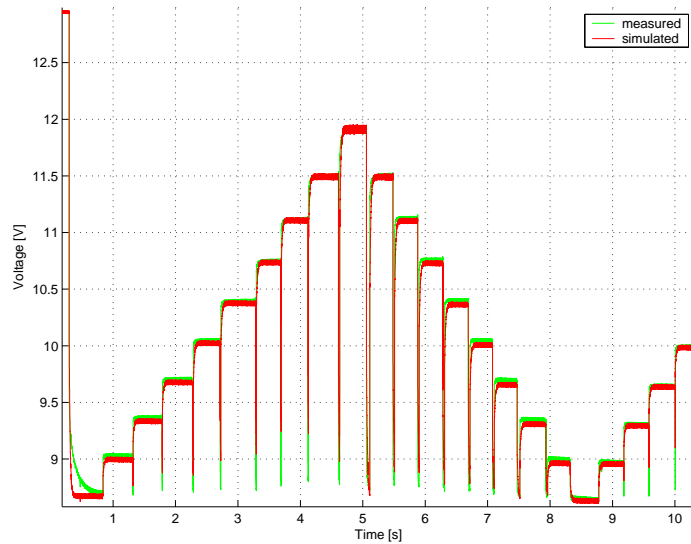
Figure 2.7: Measured and simulated voltage over a 175 Ah battery at $+20°$C.
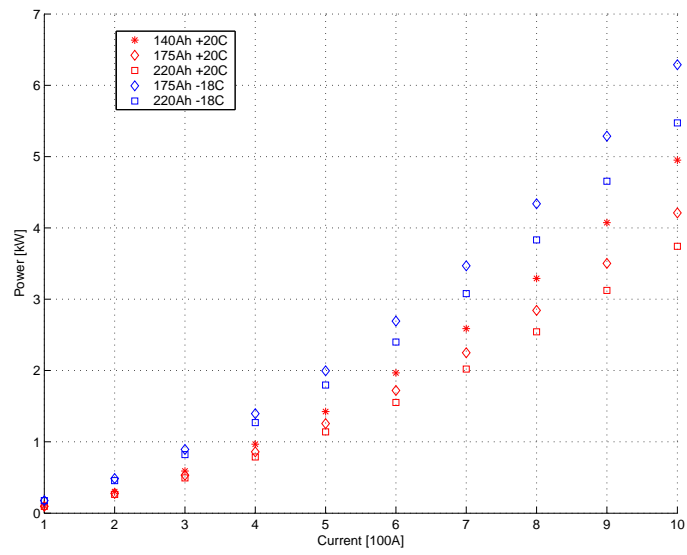
Figure 2.8: Power loss in batteries.

Chapter 3

Starter motor

3.1 Overview

The starter motors are electrical motors used for starting vehicles with internal combustion engines. In this chapter the starter motor is in focus. A basic description, theory and some features of starter motors are discussed. Related work is presented with two different starter models. Thereafter the starter model for this thesis is described. Finally tests and suggestions for future work are presented.

3.2 Introduction

The starter motor's purpose is to use the energy stored in the battery to rotate (give energy to) the combustion engine in the vehicle until the combustion engine is capable to run by itself. The starter motor will from now only be referred to as starter.

In most heavy trucks the starter is placed at the flywheel of the combustion engine. This thesis studies three different starters from the supplier Bosch. The starters are called JE, GVB and EVB. All starters are mounted in the same way and are geometrical compatible.

Scania's generation four trucks all carry a JE starter, except the old 9 litre combustion engine. The new generation of heavy trucks have a GVB starter if the engine is a V8, otherwise an EVB starter. Complete data for the EVB starter could not be found so models have only been built for the JE and GVB starter.

In figure 3.1 a starter can be viewed. When the starter switch is operated the pull-in and the hold-in windings of the solenoid are energized, connection 50 draws current. The solenoid armature pulls the engaging lever and thereby pushes the pinion towards the ring gear on the combustion engine's flywheel. When the pinion reaches the end of its travel the switch in the solenoid is
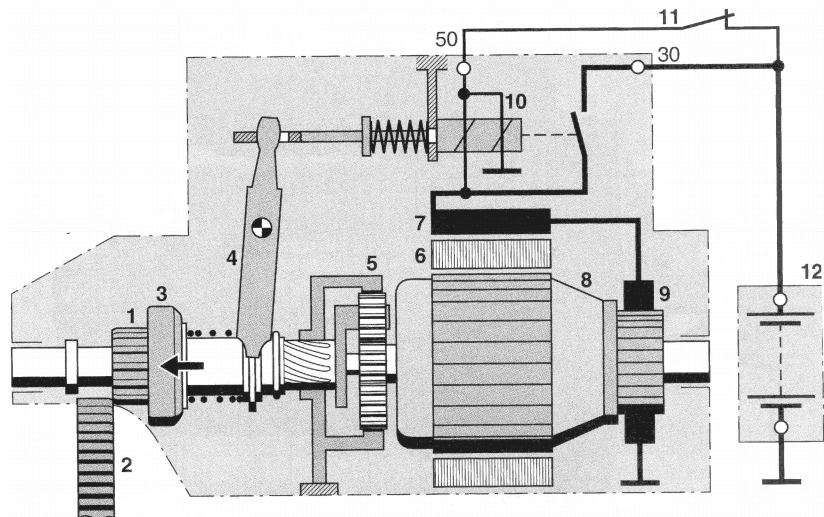
1: Pinion

2: Ring gear

3: Freewheel (overrunning clutch)

4: Engagement lever

5: Planetary gear

6: Pole shoe

7: Excitation winding

8: Armature

9: Communicator with carbon brushes

10: Solenoid switch with pull-in and hold-in windings

11: Starter switch

12: Battery

30: Electric power supply connection

50: Electric control connection

Figure 3.1: Basic diagram of starter [8].

closed. The starter motor is now energized, connection 30 starts to draw current and the starter motor starts to run.

If the pinion runs faster than the armature the freewheel breaks the connection between the pinion and the armature shaft. This protects the armature from damage. The pinion returns to its initial position only when the starter is switched off.

3.3 Theory

All studied starters are series-wound electrical motors — the excitation and armature windings are connected in series. A strong magnetic field is generated by the very high armature current when the starter motor starts under load. Thus series-wound motors develop a high initial torque, which drops sharply as the motor speed increase. These characteristics make the series-wound motors suitable as starters.

More information on these motors can be found in [20]. Figure 3.2 is a schematic description of a series-wound motor.

The windings and physical properties of the motor produce a physical variable called $K\phi$. $K\phi$ is ideally described by two functions (see figure 3.2 for key to symbols):

$$e_a = K\phi\,\omega$$
$$T = K\phi\,i_a$$

Where $K\phi$ depends on the current as a non-linear function. Using above equations and with reference to figure 3.2 the following equations can be derived:

$$v_t = R_b i_a + R_s i_a + L_s \frac{\partial}{\partial t} i_a + R_a i_a + L_a \frac{\partial}{\partial t} i_a + e_a$$
$$= (R_b + R_s + R_a)i_a + (L_s + L_a)\frac{\partial}{\partial t} i_a + K\phi\,\omega$$
$$M = T - T_f = K\phi\,i_a - T_f$$

In reality none of these physical properties are constant and the accuracy of their description is the choice for the developer of the model. The model may also include the characteristics of the starter's solenoid.

For further studies of starters the folder [8] is recommended and the book [20].
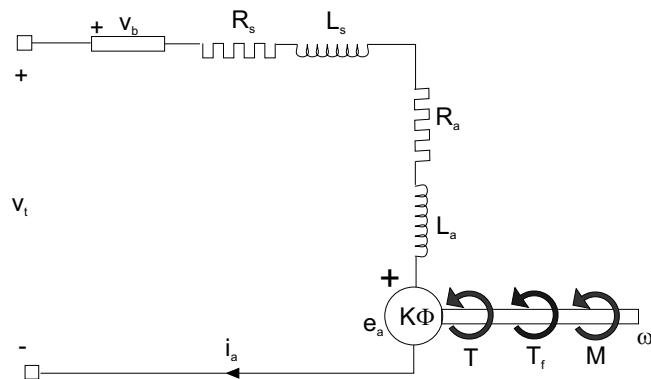
v_t: starter voltage over terminals

i_a: current through starter

v_b: voltage over the brushes

R_s: resistance of excitation winding

L_s: inductance of excitation winding

R_a: resistance of armature winding

L_a: inductance of armature winding

e_a: induced voltage (back emf) from the rotating armature

T: torque produced by the motor

T_f: torque losses due to friction

M: torque out from the starter at the pinion

ω: rotating speed of the armature

Figure 3.2: Schematic series-wound motor.

3.4 Related work

In starting system models the battery is often not modelled. As a result no electricity is modelled and the starter is described by:

$$T = C_1 e^{-C_2 N}$$

T: starter torque

N: rotating speed of the combustion engine's flywheel

C_1, C_2: constants based on the starter characteristics

This model is for example used in the papers [5], [14], [13].

When the battery is used in the simulation a more advanced model of the starter is necessary. The papers [4], [11] and [16] all use the same advanced starter model.

From steady state starter data the starter motor torque T_s and the induced voltage E_b can be approximated by:

$$T_s = \begin{cases} K_{t1} I_a^2 + K_{t2} I_a + K_{t3} & \text{for } I_a \geq I_{a0} \\ 0 & \text{for } I_a < I_{a0} \end{cases}$$
$$E_b = \log(K_{e1} I_a^2 + K_{e2} I_a + K_{e3}) \omega_s$$

I_{a0}: current threshold for armature to overcome friction losses

ω_s: motor speed

The drawback with this model is that the K parameter is divided into two, K_e and K_t.

All models of starters also have an inertia property. This is because although the starter's inertia is always small compared to the combustion engine's inertia, the ring gear transforms the inertia to a much higher value.

The paper [16] is very interesting for anyone interested in starters. The paper compares simulations of a series-wound starter and a permanent magnet starter (the excitation winding is replaced with permanent magnets, see figure 3.1). It also discusses the properties of gear reduction (see chapter 3.6.1 for gear reduction using a planetary gear).

3.5 Model

Dymola's simulation environment makes it possible to use a different model than described in the related papers. The model used in this thesis is based on

a model previously developed by Niklas Pettersson at RESC, Scania. Figure 3.3 shows the starter model.
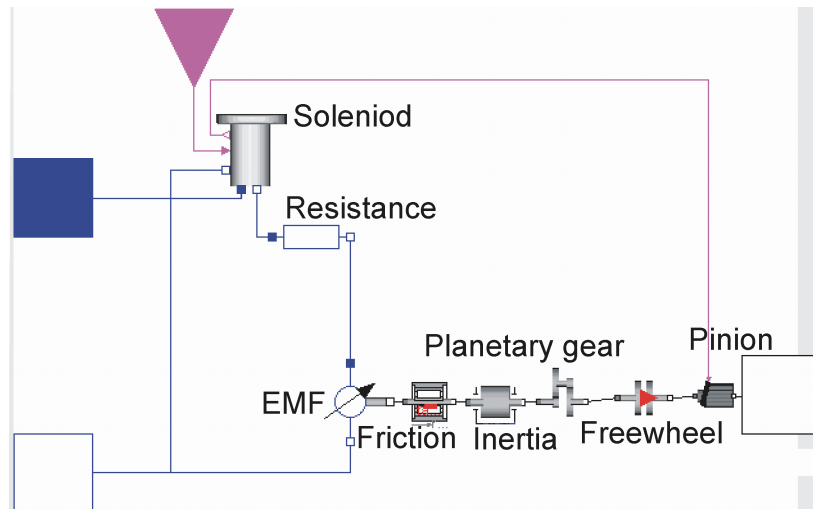
Figure 3.3: Starter model from Dymola.

All inductance is neglected. Bosch does not supply any inductive data and the winding loops are so few in the starters that the inductance probably does not affect the simulation at its present level. In the starting system the absolutely largest time-constant is the inertia. Electrically reactive components of the starter and batteries only affect the simulation at the initial peak of electric current. The peak is well outside of the models' area.

3.5.1 Interfaces

The model has four interfaces to the rest of the simulation; one start/engage Boolean connection controlling the starter switch, electrical environment plus and minus connections and a shaft connection modelling the pinion.

3.5.2 Solenoid

The solenoid in the model is a switch combined with a current sink. The switch models the state when the pinion has reached its engaged position and terminal 30 draws current. When the pinion is engaged the Boolean out port of the solenoid reads true. The travel of the pinion is modelled as instant and therefore the pull-in winding is of no interest. The hold-in winding is modelled as a current sink with current as specified in the data for the respective starter.

3.5.3 Resistance

All resistance of the starter is collected in one component. The resistance is modelled as independent of current. It depends only on starter version and outer temperature.

3.5.4 EMF

The EMF is the motor component. It holds the equations of an ideal electrical machine:

$$v = K\phi\omega$$
$$\tau = K\phi i$$

Where v is the voltage over the component, i is the current through the windings, τ is the produced torque and ω is the rotational speed of the motor armature. $K\phi$ depends on current and is tabulated for different starter versions. The variable names used here correspond to the ones used in the Modelica model.

3.5.5 Starter friction

All mechanical losses of the starter are collected as a torque loss in the starter friction. The value is independent on the rotational speed and depends only on outer temperature and starter version.

3.5.6 Inertia

All inertia of the starter is collected in this component. The value depends only on the starter version.

3.5.7 Planetary gear

The planetary gear is ideal and the ratio value depends on the starter version.

3.5.8 Freewheel

The freewheel makes it only possible to transfer torque from the EMF to the pinion. If the pinion moves faster it is disconnected and runs free. The freewheel is modelled as an ideal component.

3.5.9   Pinion

The pinion is an ideal gear connected in series with an ideal clutch and describes the gear ratio from the starter to the ring gear of the combustion engine. When the Boolean in port of the pinion reads true the clutch is engaged and thereby also the pinion.

The ratio value of the pinion gear depends on the starter version.

3.5.10   Starter data

For tabulated starter data used for the models, see table 3.1, 3.2 and 3.3. It can be seen that the resistance increases with temperature. The friction is a more complex phenomenon.

Version	Mechanic power	Weight	Planetary gear ratio	Inertia at pinion (at armature)
JE	6.7 kW	19 kg	1	0.00321 (0.00321) kgm^2
GVB	6.0 kW	12 kg	3.16	0.0127 (0.00127) kgm^2
EVB	5.5 kW	9.5 kg	4.15	0.0117 (0.00068) kgm^2

Table 3.1: Starter data supplied by Bosch.

Version	Resistance; $-18°$C, $+20°$C	Friction; $-18°$C, $+20°$C
JE	6.0 mΩ, 7.1 mΩ	7.6 Nm, 5.7 Nm
GVB	6.7 mΩ, 7.2 mΩ	2.3 Nm, 2.4 Nm

Table 3.2: Starter data found by optimization (see chapter 3.7.2).

Version	Total mass	Copper mass
JE	19 kg	2.65 kg
GVB	12 kg	1, 27 kg
EVB	9.5 kg	1, 3 kg

Table 3.3: Starter masses.

3.6   Tests and supplier data

The only successful starter tests were the tests of the complete starting system. The tests are described in chapter 5.6 and in detail in appendix A.1.2. Some of the non successful tests are mentioned in appendix A.2. From these tests it is not possible to build a starter model. The tests have been used for evaluation of the starter models and to compare with the data available from the starter

supplier, Bosch. The results from the tests also provide valuable information for what regions of the starter model to focus on; what regions the model has to be as close to reality as possible and in what regions do flaws have little effect.

3.6.1 Data from Bosch

The starter model is built from data supplied by Bosch. The used data is the inertia, solenoid currents and graphic presentation of the starters' characteristics, see figure 3.4.
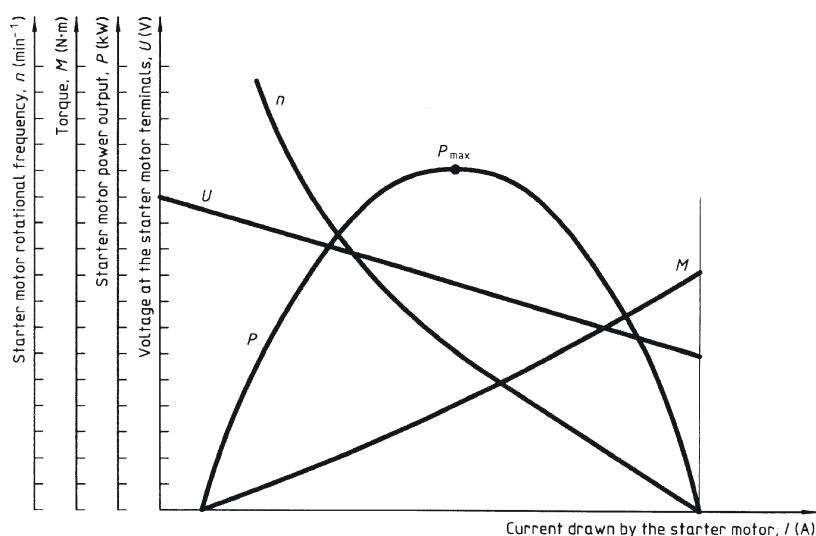
Figure 3.4: Starter characteristics from ISO standard 8856 [23].

A complete description of the procedure the tests followed can be found in an ISO document [23], but the tests can be done in a few different ways. The most interesting choice is that it is possible to measure at discrete torque loads or to do a continuous measurement with increasing torque. How Bosch do is not known and a visit to their test facility would be necessary for obtaining a good understanding of their procedure. In the graphic presentation are minimum, mean and max curves plotted. The mean curves have been used in the models.

The two new starters GVB and EVB have a planetary gear. This feature has a lot of implications. For the GVB starter the ratio is a little over three, therefore the armature has to have three times the speed and the inertia is nine times multiplied. The new starter motors are smaller than the older JE starter, but still have a lot higher inertia (see table 3.1).

3.7   Simulation and model adjustment

Simulations and tests for different starter models were mostly done in Matlab. Results from Matlab were then transferred to Dymola.

3.7.1   Solenoid

The value for the current sink was fitted to data supplied by Bosch for the GVB [7]. This value was also confirmed in tests. For the JE starter the value was found in [6].

If the model should be enhanced with the time to move the pinion, model example can be found in [11] and values can be found in the results from the tests in engine cell K2.

3.7.2   Resistance, friction and $K\phi$

The resistance of the starter is approximately modelled as constant. Many different electric losses are collected in this resistance, for example voltage loss over the brushes, the contact resistances at the terminals and the resistances of the two windings.

The friction is also approximately modelled as constant due to the difficulty in measuring a dynamic friction and the aim to keep the model as simple as possible.

By optimization constant values for the losses were found. The two formulas for $K\phi$ was used on data given from Bosch (see chapter 3.3 and 3.6.1) and the difference was minimized, e.g.:
$\min_{R,T_f} [(v_t - Ri_a)/w - (M + T_f)/i_a]$.

Following, a $K\phi$ vector was created as a mean value from the two calculated $K\phi$, see figure 3.5. The $K\phi$ vector proved to be independent of temperature, and only R_s and T_f depend on the temperature. The values are best fitted for currents from 300 A to 600 A at $+20°$C and 600 A to 1000 A at $-18°$C.

The result reveal a small model error in both M and v_t as can be seen in the figures 3.6 and 3.7.

3.8   Future work

- The electrical losses in the starter depend on the dynamic starter temperature. This is an important characteristic for further investigation. The temperature increase is also an important factor in itself that should be looked into. With the new starters' lesser mass, heat transfer is less and the starters become hotter. The high heat of the starter could in itself prove to be a limiting factor.
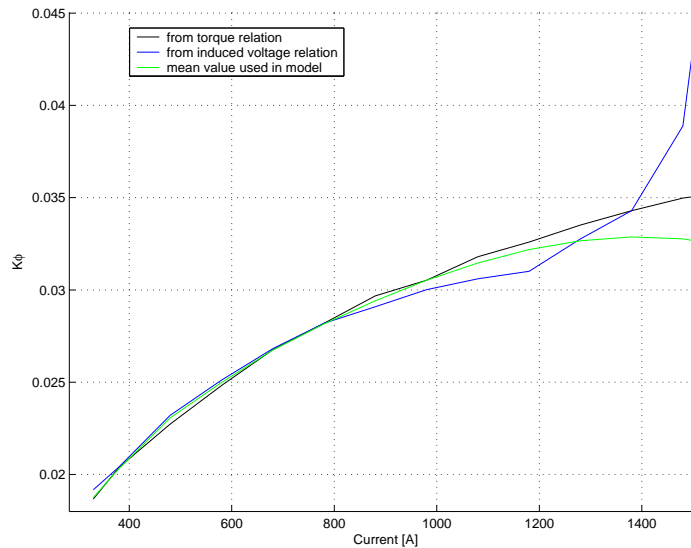
Figure 3.5: $K\phi$ curves for the GVB starter at $+20°$C.

- Better models could probably be developed if a better understanding of Bosch's test procedure could be obtained. A visit to their test facility and evaluation could prove very useful.

- Further investigation of the initial peak of current, before the starter motor starts to turn, could be looked in to. The peak is a chock for the battery and therefore interesting for this work.

- The freewheel is modelled as ideal, a better model could be developed.

- Find relation between the losses (friction and resistance) and $K\phi$ for different sizes of starters. If results are obtained in this area, an optimization of size of the starter motor could be looked upon.
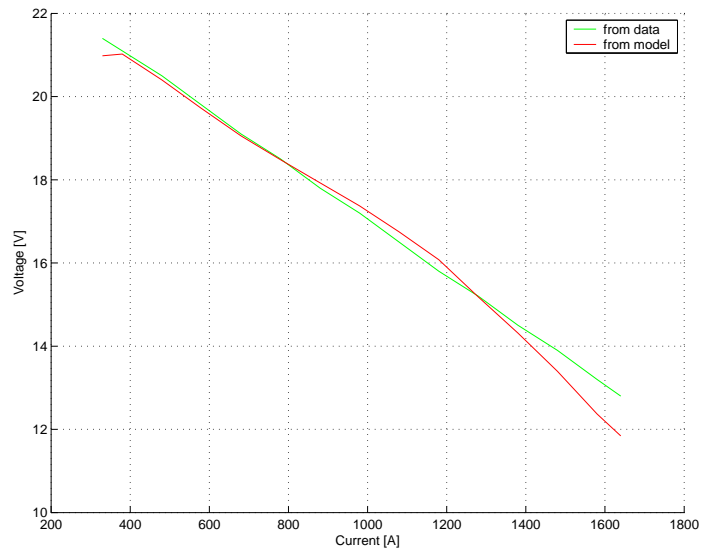
Figure 3.6: Induced voltage in the GVB starter at $+20°$C.
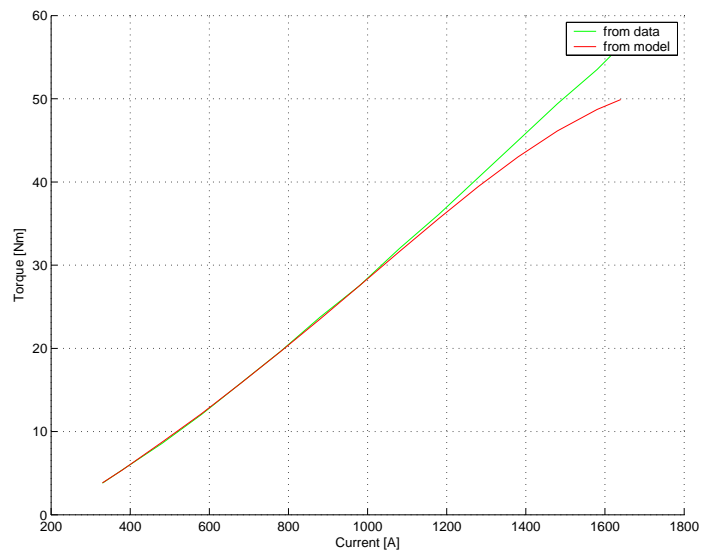
Figure 3.7: Produced torque in the GVB starter at $+20°$C.

Chapter 4

Combustion engine

4.1 Overview

The combustion engine is of course one of the major parts of a heavy truck — many people would say it is the heart of the vehicle. In this chapter the focus is on the combustion engine. The basic functions and theory of the combustion engine are described. Four papers with their engine models are shortly mentioned. Thereafter the combustion engine model for this thesis is described. Finally tests, simulations and suggestions for future work are presented.

4.2 Introduction

The purpose of a vehicle is to travel. The engine is the component which transforms stored energy into movement. Only four-stroke diesel engines will be discussed in this thesis and of course Scania's combustion engines are in focus.

Scania has today four different sizes (swept volume) of engines in production; 9-, 11-, 12- and 16-litre. The 16-litre engine is a V8, the 9-litre is the new inline five cylinder engine and the others are inline six cylinder engines. Notable is that all these engines have the same unity cylinder. More information of Scania's engines can be found at Scania's homepage www.scania.com. A schematic description of an internal combustion engine can be found in figure 4.1.

Scania only manufactures four-stoke diesel engines. A diesel engine is a compression ignition engine, e.g. the rise in temperature and pressure during compression is sufficient to cause spontaneous ignition of the fuel (diesel). The four-stroke operating cycle can be explained with reference to figure 4.2.

The starting process of a combustion engine has two very different states. One is when the engine is driven by the starter and the other when the engine
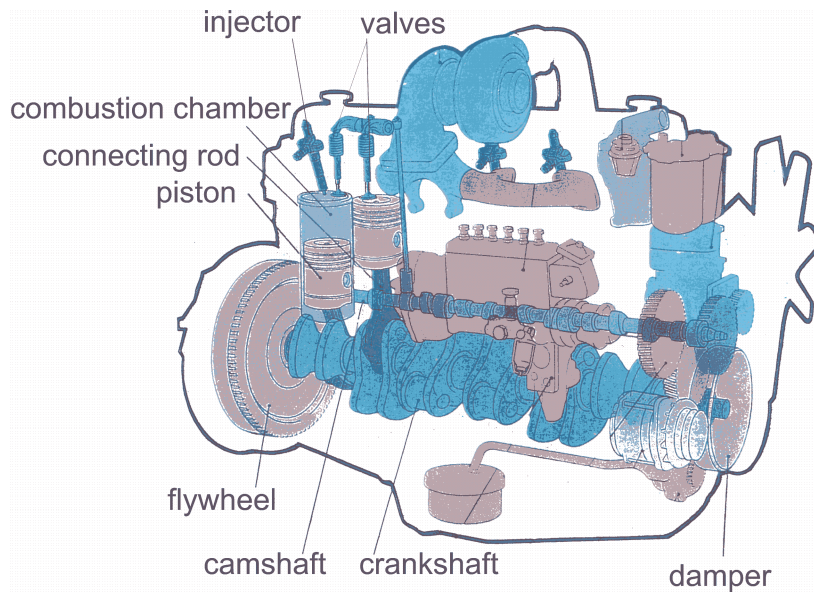
Figure 4.1: Schematic figure of internal combustion engine.

has started to run by its self, but not yet reached stable idle speed. When the combustion engine has reached idle speed the starting process is over.

The state when the combustion engine is driven by the starter is called cranking. The model in this thesis only handles cranking.

For further basic studies of combustion engines the site `http://www.-tpub.com/content/engine/14037/css/1403789.htm` is recommended, it is an internet site containing online books from the US Navy. For more advanced questions the book [22] is better.
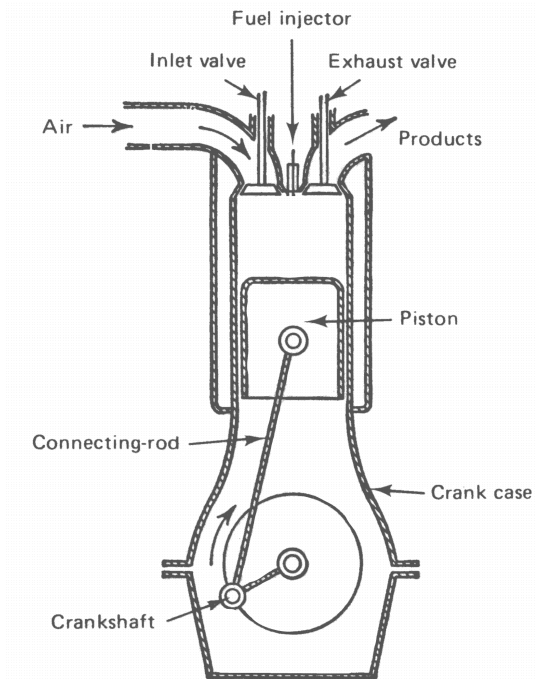
Figure 4.2: A four-stroke engine [22].

The induction stroke: The inlet valve is open, the piston travels down the cylinder, drawing a charge of air.

The compression stroke: Both valves are closed, and the piston travels up the cylinder. As the piston approaches top dead center ignition occurs if conditions are upheld. The fuel is injected at the end of this stroke.

The expansion, power or working stroke: Combustion propagates throughout the charge, raising the pressure and temperature and forcing the piston down. At the end of the stroke the exhaust valve opens. In this thesis combustion never takes place, but much of the energy in the compression is regained.

The exhaust stroke: The exhaust valve remains open, and as the piston travels up the cylinder the remaining gases are expelled.

4.3   Theory

In [22] some processes and components which might be necessary to model
for a turbocharged diesel engine are listed (selected):

- The compressor (and inter-cooler if fitted).

- Unsteady-flow effects in the induction system.

- Flow through the inlet valve.

- Air motion within the cylinder.

- Dynamics of the injection system.

- Fuel jet interactions with the trapped air to form a spray.

- Combustion (including the effects of the ignition delay and turbulent
  compression).

- Heat flow within the combustion chamber.

Many of these processes are very hard to describe and engine models rely
heavily on experimental data and empirical correlations. In this thesis only
the starting process is regarded and since the model used does not handle
combustion, it is further limited to cranking. During cranking the combustion
engine can be viewed as a load to the starter.

The net torque (during cranking this is the torque the starter has to pro-
duce) is the sum of gas pressure torque (rise and release of pressure in cylin-
ders), inertia torque (of the entire engine) and friction torque (all mechanical
losses).

The friction torque describes the energy losses of the mechanical parts of
the engine. The losses include friction in all bearings, work to open valves
and injectors, work to drive the oil pump, etc. There is no general rule how
to describe these complex processes. Some methods are described in chapter
4.4 and the choice for this thesis in chapter 4.5. What is absolutely certain
is that the friction is highly dependent on the oil and the temperature of the
engine.

The inertia torque is the sum of all inertia of the engine from flywheel,
damper, etc. Included in the inertia is the kinetic energy of the reciprocating
parts (piston assembly, etc.). This energy is neglected (due to low speed), cal-
culated as an average, described as moving masses, or a mix of the description
ways.

The pressure torque is derived from the complex processes resulting in
a pressure force on the piston. The theories describe the gas flow into the
cylinder through the intake system, the processes in the cylinder and the gas
flow out of the cylinder through the exhaust system. Since the model of this
thesis does not handle combustion the processes in the cylinder are described

by basic thermodynamics. Notable is that the compression torque varies more with fewer cylinders. This is further discussed in the paper [14]. When combustion and valve flow is needed more complex phenomena needs to be described. Theory for this can for example be found in the related work or in [22].

For further studies of combustion engines [22] is recommended.

4.4   Related work

Very short descriptions of the engine models of four related papers are presented here. All engines are four-stroke diesel engines. How the engine is modelled is of course highly dependent of the goal of the total simulation and these papers are further discussed in chapter 5.4.

In [5] a single-cylinder engine is modelled during cranking and starting. Combustion is included and the engine can run up to idle speed. Thermodynamic and combustion equations describe the processes inside the combustion chamber, including blow by and gas to wall heat transfer. The gas exchange process, with the intake and exhaust manifolds, is described with equations for infinite plenums, thus neglecting dynamic effects due to pressure waves. The friction is classified under two categories; piston assembly friction and crankcase assembly friction, each category with three sub components. The inertia is calculated as sum of the rotating parts and a reciprocating torque.

[14] contains models of eight, four and three cylinder engines. No combustion is simulated. Heat losses and blow by are neglected. The friction is taken to be constant for each degree of crank rotation, independent of speed. The inertia is only the rotational parts and the reciprocating parts are neglected.

In [4] a four cylinder engine is simulated. The engine model contains combustion and the engine runs up to idle speed. Gas dynamics around the manifolds are simulated, but pressure waves are neglected. So are also heat losses and blow by. Friction is modelled from a regression model based on test data and theoretical torque balance. The difference between torque used for acceleration and torque provided by the starter, plus the cylinder pressure torque, is the friction torque.

In [13] an eight cylinder engine is simulated. The combustion and gas dynamic processes have the same properties as the single cylinder engine in [5], but are based on somewhat different expressions. The friction is modelled as in [4].

4.5   Model

The model used in this thesis is based on a model previously developed by Niklas Pettersson at RESC, Scania. No combustion or fuel injection is sim-

ulated. Fuel injection influences the combustion chamber and is further discussed in chapter 4.8. Blow by is not modelled, but energy losses in the combustion chamber is modelled as gas to wall heat release. The engine is perfectly balanced and this affects the simulations results.
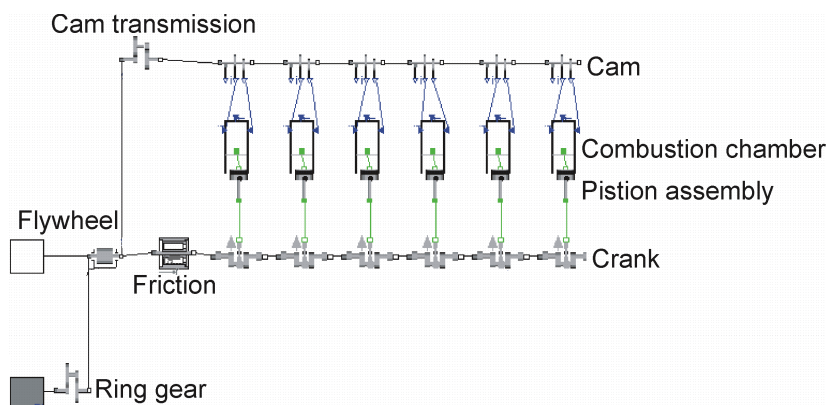
Figure 4.3: Internal combustion engine model with six cylinders from Dymola.

The base engine of this thesis is the DT12 02 engine used in the cell tests. The DT12 02 is an inline six cylinder internal combustion engine with 470 hp. The two other engines used in the simulations, a five cylinder (ICE5) and an eight cylinder (ICE8) engine, are models with changed number of cylinders and scaled friction. The ICE8 engine is supposed to model a V8 engine. In the paper [12] a V-engine has 15% lower friction than corresponding inline engine. Thus the friction of the ICE8 engine is determined as $0.85 \cdot 8/6$ of the DT12 engine's friction.

The oil quality has a prominent effect on the friction. There are no options for different oils in the models.

The inertia and reciprocating masses are taken from tabulated data for the D12 (six cylinders), D9 (five cylinders) and D16 (eight cylinders) engines.

4.5.1 Interfaces

The combustion engine has only two interfaces. Both are mechanical connections to the flywheel. One is for the clutch and the other for the starter at the ring gear.

4.5.2 Ring gear

The ring gear is an ideal gear with the ratio of the number of teeth on the ring gear. The component together with the starter's pinion describes the ratio between the starter and the crankshaft.

4.5.3 Flywheel

The flywheel describes the total inertia of the engine. The inertia includes the bay (crankshaft and big end of connecting rod), damper package, fan and flywheel. The data was supplied by Johan Lundqvist NMBP, Scania.

4.5.4 Cam transmission

The cam transmission connects the crankshaft to the camshaft with a ratio of two.

4.5.5 Friction

The friction of the combustion engine is composed of tabulated data estimated from system tests and simulations.

For the model in this thesis a tabulated friction, dependent on speed, crank angle and temperature would be a good level of complexity. With the accessible test equipment this was not possible to measure, so the friction is only a function of speed and temperature. This is further discussed in chapter 4.7. The scaled friction of the different engine models was discussed in chapter 4.5.

The friction depends on temperature and crankshaft speed.

4.5.6 Cam

The cam components describe the behaviour of the camshaft. Signals for normalized intake and exhaust valve lifts are available from the cam component.

4.5.7 Combustion chamber

The combustion chamber models the cylinder, the cylinder head and the processes inside the cylinder. No combustion is possible in the current implementation of the component. Blow by is not modelled, but energy loss during compression is modelled as gas to wall heat loss. The gas in the cylinder is assumed to follow two-atomic ideal gas properties and is modelled with thermodynamics theory. The gas to wall heat release is modelled as suggested by Hohenberg [10].

4.5.8 Crank

The crank components describe the behaviour of the crankshaft. The forces from the translational moving pistons are transferred to the rotating crankshaft.

4.5.9   Piston assembly

The piston assembly component models the reciprocating masses of the piston and the small end of the connecting rod. The masses are taken from tabulated data supplied by Johan Lundqvist NMBP, Scania.

4.6   Tests

Test of an inline six cylinder engine were made at engine cell K2, STC.

Torque to pull the engine from 10 rpm to 300 rpm was measured, both with and without compression (injectors removed), and at both $+20°C$ and $-18°C$. These measurements all proved far from simulation results and this is further discussed in appendix A.1 and the now following chapter 4.7.

4.7   Simulation and model calibration

Instead of direct measurements the friction of the engine had to be estimated from systems tests compared with simulations. These tests are described in chapter 5.6 and appendix A.1. The model calibration is described in chapter 5.7.

A number of different friction models were tried. Finally a friction depending on rotational speed and temperature was found to describe the system best. The speed dependence was estimated from the torque cell tests, since the system tests could not be used for this value due to the too small speed variations. The way to determine the engine friction results in an over-estimation; energy losses are present all over the system, for example in the pinion ring gear connection. Further tests must be done to determine where the losses are and where to place them in the total system simulation.

4.8   Future work

- The first thing to add to the model is fuel injection. Fuel injection has probably a significant effect since it cools (by going from liquid to gas), heats (by adding mass to the combustion chamber) and seals the chamber (decreases blow-by). To be able to verify any fuel injection model in tests, a pressure sensor is needed. The pressure sensor must be dynamic and at the same time be exact at the low cranking pressure as well as withstand the high combustion pressure and temperature. This is further discussed in appendix A.1

- New friction measurements should be done with better equipment, so the friction can be better estimated and dependent on crank angle and speed. Tests can also be done to examine the effects of different oil qualities.

- A blow by process could be added to the model of the combustion chamber.

- More exact gas dynamic processes around the valves could be added to the combustion chamber or built as a cylinder head component.

- The engine modelled in the thesis is perfectly balanced. Better geometrical models could be developed. Also work done in the cylinder head by the camshaft (open valves and injectors) could be added.

- Finally the model could be increased to run up to idle speed. For this end the combustion chamber must handle combustion and the increased speed of the combustion engine would also puts new demands on the friction model.

Chapter 5

Starting system

5.1 Overview

Now it is time to collect all the components of the previous chapter and put together a full starting system. In this chapter a full starting system is described. The starting system is defined and the theory described. Five papers of starting system simulations are briefly looked upon. Thereafter the model of this thesis with its components described. Tests and simulations of the tests are presented with discussions. Finally a few suggestions for future work are mentioned.

5.2 Introduction

A full starting system is composed of battery, starter and combustion engine. The modelling of the starting system depends of course completely on the goal of the simulation. This goal makes it necessary for a limited top-down design. At the same time the simulation environment often uses a bottom-up design, for example object oriented heritages.

   The demand for the simulation results is to be good enough with as simple a model as possible. The more complex the model is, the harder it is to verify that it really simulates the reality.

5.3 Theory

The theory for the complete system is built up by all its components. When building the complete system all the subsystems must be considered — some properties are necessary to describe and some are less important.

   An important characteristic is a reference factor to evaluate engine start ability. In [5] the following is suggested:

- Required cranking time

- Time from starter on to combustion can start

- Cranking torque and smoke measurements

- Time from starter on to starter off

- Time from starter on to idle speed

In [17] "Time to specific cranking speed" is added to the list and for starter evaluation "the first peak of RPM reached".

For a cranking model the first ignition would be a good reference point. This is very hard to calculate and cranking speeds are a better focus at the present complexity of the model used in this thesis.

5.4   Related work

All the related papers describe the starting process of systems with four-stroke diesel engines.

In [5] a mathematical model is developed to study the transient behaviour of a four-stroke single cylinder engine. The model simulates the thermodynamic cycle of the engine and includes models for the intake and exhaust gas flow processes, combustion, heat transfer, friction, blow by, and engine mechanical dynamics. The model simulates the time from starter until the engine reaches idle speed. No battery or electrical processes of the starter are simulated.

[14] studies the crank speed variations for engines with different number of cylinders and design; inline or V. Focus is on compression time and its influence on temperature and pressure inside the combustion chamber. No battery or electric parts of the starter are modelled. The model is based on energy theory and do not contain combustion. A discussion is made of possible design changes, especially with focus on the starter's characteristics.

[17] describes a general mathematical model of an engine with a starter motor. The models are only schematically described, except the engine's mechanical dynamic and friction. The paper investigates three different starters, change of engine rotating inertia, effect of reduction ratio between the starter and combustion engine. The engine used in the simulation is a two-stroke single cylinder spark ignition engine, but the results are clearly useful for other types of combustion engines.

[4] describes a full starting system with battery, starter and combustion engine. The goal of the simulation is to be a tool for transient and systematic analysis of engine starting. Comparisons between simulation and tests are mostly discussed, but also a few variable quantities, which are hard to measure, found in the simulations.

[13] develops a mathematical model of engine and the starting system during cold start at $-32°C$. No battery or electric parts of the starter are modelled. The simulations investigate the effects of blow by, intake air temperature increased by flame heater, initial cylinder wall temperature and heat loss in the cranking process.

5.5 Model

The starting system of this thesis is composed of the components described in the previous chapters; a battery box with two batteries, a starter and a combustion engine. A few components are added and described in this chapter.
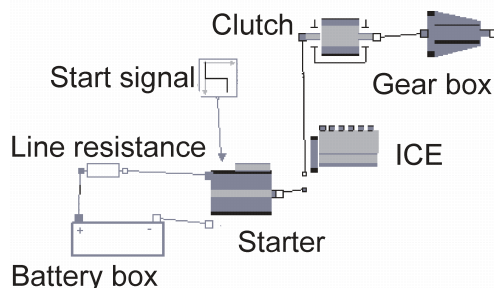
Figure 5.1: Starting system model from Dymola.

The Dymola model of the starting system can be found in figure 5.1. The components are connected and an electric line resistance is introduced between the starter and battery box. Losses in the connection between starter and the combustion engine's ring gear are neglected. To the flywheel a clutch and a gear box component is connected.

5.5.1 Clutch

The clutch component models the inertia of the clutch's disc, pressure plate and back end. The values are taken from tabulated data for the manual clutch package for the corresponding engines, supplied by Johan Lundqvist NMBP, Scania.

5.5.2 Gear box

When a truck starts the clutch is engaged. The gearbox is thereby also rotated and in neutral state. The gearbox is composed of inertia and friction. These values were hard to find and had to be approximated from data supplied by Magnus Freij NTM, Scania. No data were given for oil quality.

5.6   Tests

Test of a system with an inline six cylinder combustion engine was made at engine cell K2, STC. In the K2 cell it is possible to perform tests in a cooled environment.

All three versions of starter motors, EVB, GVB and JE, was one after the other mounted on the combustion engine. The system was cranked for twenty seconds and the following was measured:

- Voltage over the starter motor.

- Current drawn by the starter motor.

- Rotational speed of the combustion engine.

- Pressure in the sixth cylinder of the combustion engine.

The tests were performed both at $+20°$C and $-18°$C. At $+20°$C the EVB used 175 Ah batteries, all the other tests were performed with 220 Ah batteries. The combustion engine was equipped according to Scania technical regulation for starter motors [1].

The torque produced by the starter was also measured, but the measurement was disturbed by the starter's magnetic field.

Detailed description of the tests can be found in appendix A.1.

5.7   Model calibration by simulation

The system tests were repeated as simulations. The inertia of the clutch in the cell was estimated by the mass and form. No gearbox was used in the tests and therefore removed from the simulation. The battery model is only made for fully charged batteries. However the number of batteries available for the tests was limited and as a result most tests were performed with not fully charged batteries. To compensate for this the line resistance was increased, but effects are still visible, mostly in the voltage response.

The simulations were used to verify the starting system model and to find a model and corresponding parameter value for the engine friction. Simulation and test results after two seconds cranking are plotted in figures 5.2, 5.3, 5.4 and 5.5.

The simulation deviations are much smaller at the $-18°$C results. One reason is that the tabulated data over the starters' characteristics. It is focused on high currents. Thus, the starter model is probably better at the high currents of a low temperature.

One interesting thing to note in these figures is the form of curves in the warm environment. The GVB starter has saw tooth looking graphs and the JE starter's shape of responses look more like the starters' responses in the cool environment. The phenomenon is more obvious in the test than in

(a) Voltage over starter

(b) Current drawn by starter

(c) Crankning speed of combustion engine

(d) Torque produced by starter
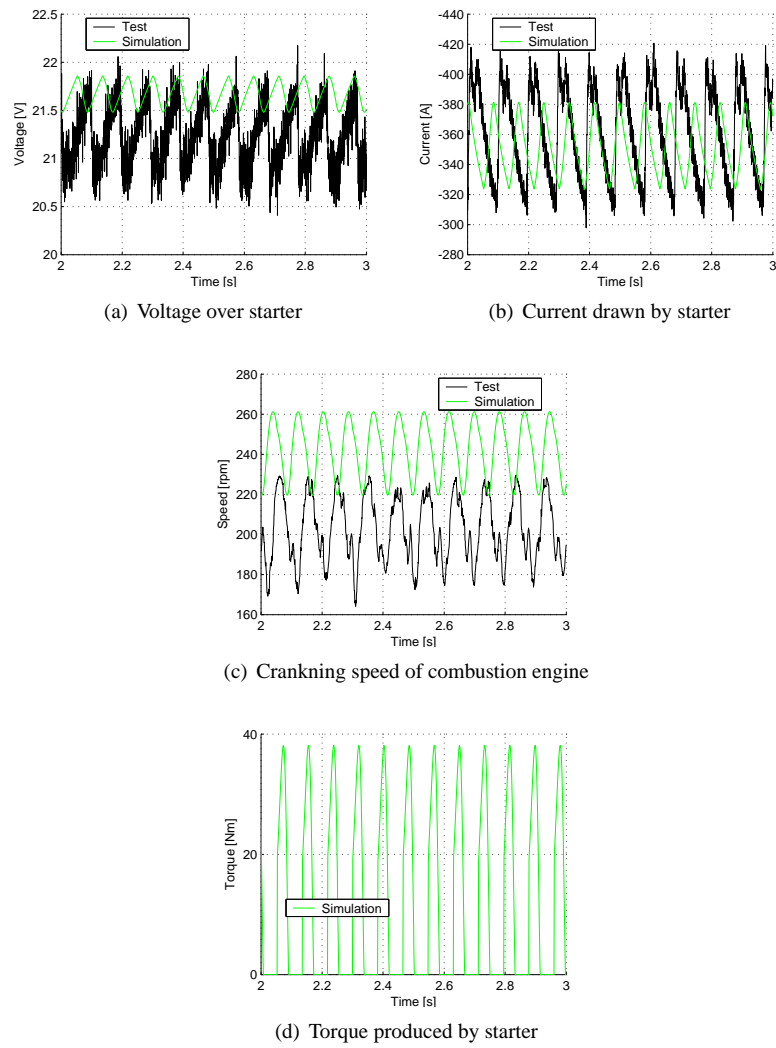
Figure 5.2: Simulated and test results of a system with 220 Ah batteries, GVB starter and DT12 engine at $+20°$C.

(a) Voltage over starter

(b) Current drawn by starter

(c) Crankning speed of combustion engine

(d) Torque produced by starter
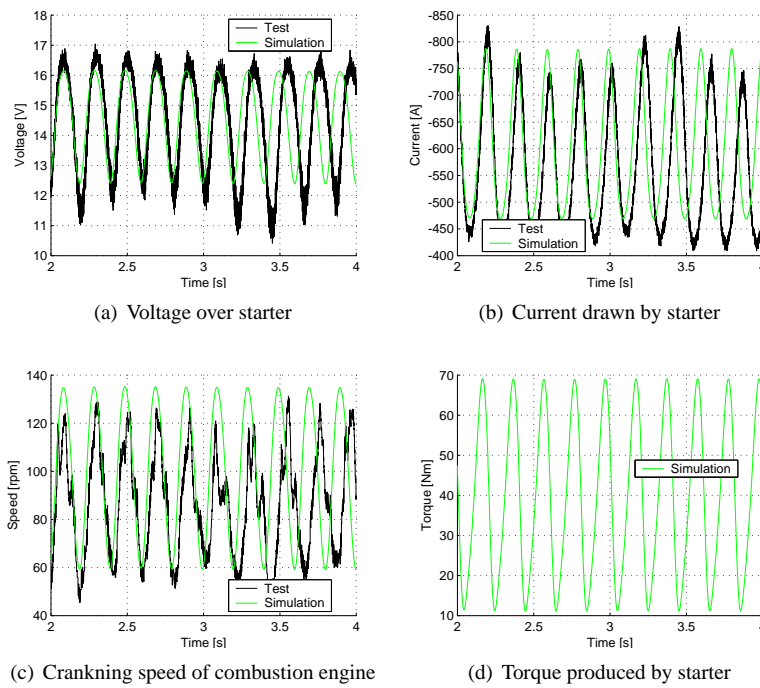
Figure 5.3: Simulated and test results of a system with 220 Ah batteries, GVB starter and DT12 engine at $-18°$C.

(a) Voltage over starter

(b) Current drawn by starter

(c) Crankning speed of combustion engine

(d) Torque produced by starter
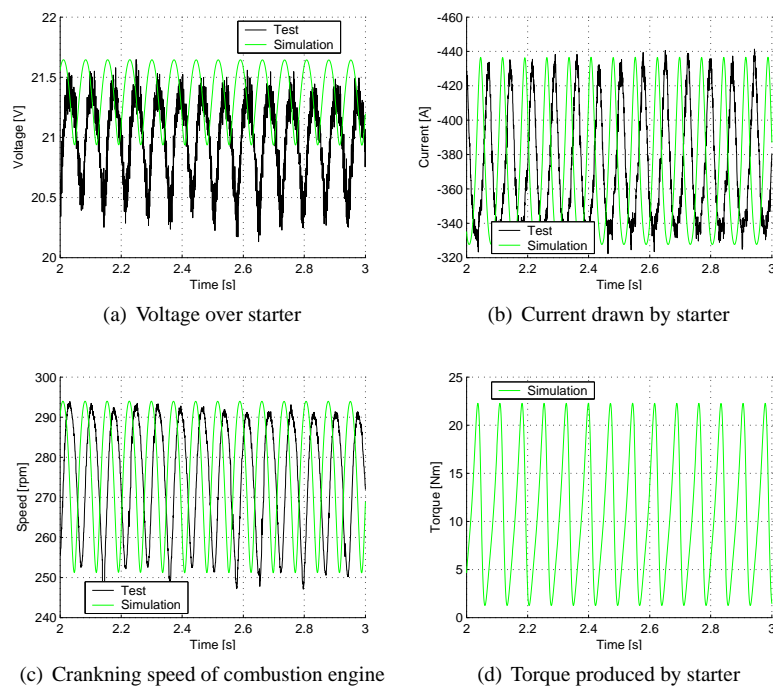
Figure 5.4: Simulated and test results of a system with 220 Ah batteries, JE starter and DT12 engine at $+20°$C.

(a) Voltage over starter

(b) Current drawn by starter

(c) Crankning speed of combustion engine

(d) Torque produced by starter
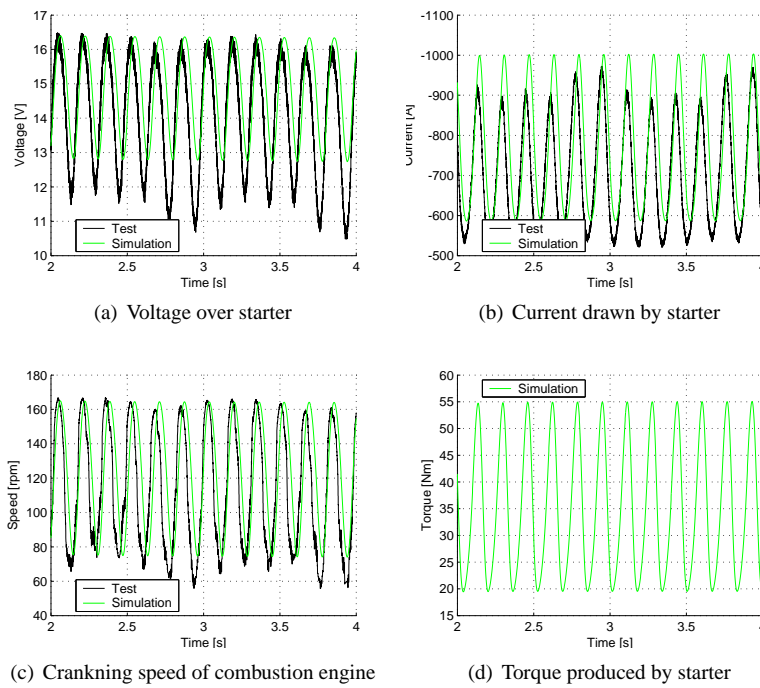
Figure 5.5: Simulated and test results of a system with 220 Ah batteries, JE starter and DT12 engine at $-18°$C.

the simulation. The reason for this in the simulation is zero crossing of the starter's pulled torque, as can be seen in figure 5.2(d).

The simulated combustion engine is perfectly balanced and the friction, including work done by the camshaft, does not depend on crank angle. When the GVB starter applies a high torque during a short time it gets more affected by irregularities in the load from the combustion engine, e.g. the engine is not perfectly balanced and the work done by the camshaft is not uniform in a crank turn. This could be an explanation for the difference in cranking speed between test results and simulation for the GVB starter system at $+20^\circ$C (see figure 5.2(c)).

5.8 Simulation

To get some feeling for the dynamics of a starting system a few simulated results are presented here. A starting system with 175 Ah batteries, a GVB starter motor and a six cylinder combustion engine is simulated at -18°C and $+20^\circ$C. The selected presented results are:

- Voltage over the starter motor.

- Current drawn by the starter motor.

- Cranking speed of the combustion engine.

- Torque produced by the starter motor.

The initial peak of the system is out of the models' calibrated range and should be looked upon with caution. In figure 5.6 the results are plotted.

5.9 Future work

Suggestions for future work on each component can be found in each corresponding section. The most important for the system as a total is to make more tests with different engines and calibrate and validate the starting system model. A better gear box model with values from tests would also improve the results.
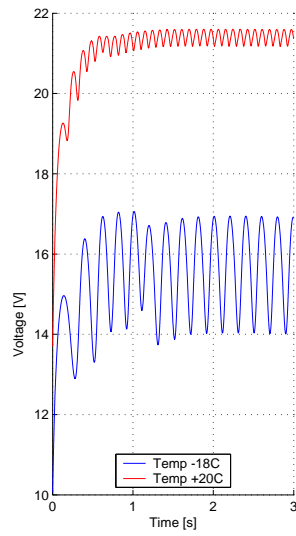
(a) Voltage over starter
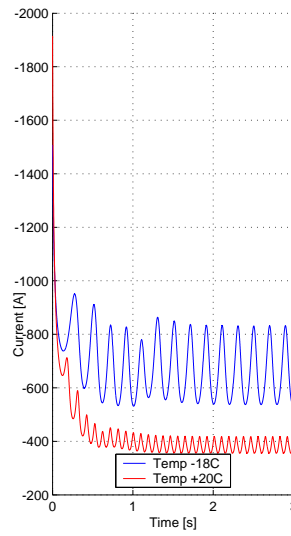
(b) Current drawn by starter
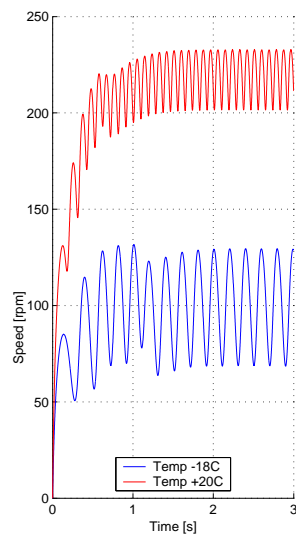
(c) Cranking speed of combustion en-
gine
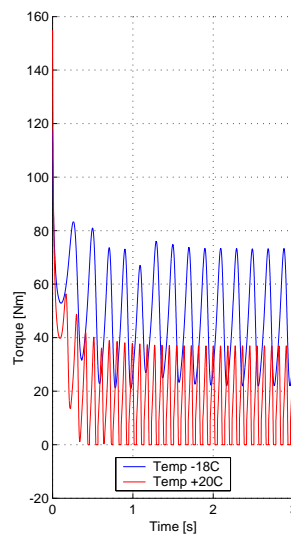
(d) Torque produced by starter

Figure 5.6: Simulation of a starting system with 175 Ah batteries, a GVB
starter motor and a six cylinder combustion engine at $-18°$C and $+20°$C.

Chapter 6

Starting system simulations

Now it is time to use the models described in the previous chapters. In this chapter four examples of possible starting system simulations are presented. Full starting systems are simulated as described in chapter 5. The simulations have been run for four seconds. Maximum, mean and minimum values from three to four seconds are presented. The variations are present due to the dynamic pressure torque, see chapter 4.3. In the power figures the max and minimum values are of lower interest and only mean values are plotted.

The selected presented results are:

- Voltage over the starter motor.

- Current drawn by the starter motor.

- Cranking speed of the combustion engine.

- Torque produced by the starter motor.

- Electric power consumed by the starter motor.

- Mechanic power produced by the starter motor.

- Lost power in the starter motor (power difference between electric and mechanic power, released as heat in the starter motor).

- Power efficiency of the starter motor. The starter motor's efficiency is not the efficiency for the whole starting system. It is only a simulation of the starter motor's efficiency.

The first simulation investigates a system with different batteries at different temperatures. The second simulation investigates the effects of combustion engines with different number of cylinders. The third simulation investigates the effects of increased electric resistance in the starting system. The fourth simulation investigates the effects of starter motor to crank shaft ratio.

51

The models of each component is described in each corresponding chapter; for the battery chapter 2.5, for the starter motor chapter 3.5 and for the combustion engine chapter 4.5.

The main thing to look at in the figures is the minimum cranking speed. The cranking speed is lowest during the compression stroke and this limits the start ability of the starting system. Another interesting value is the lowest voltage. If the voltage becomes too low over the electric system the other electric components of the heavy truck, e.g. computers and controllers, will fail. The mean drawn current is also of special interest since it is a good measure of the used capacity for starting, but the phenomenon is more complex involving for example the cranking speed.

All the simulations have the following interesting results in common:

- The JE starter draws more current and uses more power.

- The GVB starter has almost always better starter efficiency and probably better efficiency for the whole starter system.

- The GVB starter has greater variations in produced torque.

6.1   Batteries and temperature

In this section a starting system with a six cylinder combustion engine is simulated. Three different simulations are presented:

- System with 220 Ah batteries at $-18°$C.

- System with 175 Ah batteries at $-18°$C.

- System with 175 Ah batteries at $+20°$C.

All the simulations are performed with both the JE and GVB starter. The results are presented in figure 6.1 and 6.2.

Some interesting things to note in these figures:

- The 220 Ah batteries have lower internal resistance then the 175 Ah batteries and thereby give a higher voltage over the starter and a higher cranking speed.

- The system with 220 Ah batteries have lower mean current and higher cranking speed than the 175 Ah batteries system. Thereby the 220 Ah batteries system not only has more battery capacity, it also very possibly uses less battery capacity for starting.

- The system with 220 Ah batteries have higher starter motor efficiency than the 175 Ah batteries system.

- In the $-18°$C simulations all variations are greater compared to in the $+20°$C simulation.

- In the $+20°$C simulation the JE starter gives a higher minimum speed than the GVB starter, but draws more current. The higher speed of the JE starter has probably no significant effect on the starting process.

- In the $+20°$C simulation the GVB starter has zero-crossing of the torque. This gives according to the comparisons with the tests an over-estimation of the simulated speed (see chapter 4.7 and 5.7), but the speed will still be high.

- In the $+20°$C simulation the GVB starter has lower efficiency than the JE starter and is has also lower mass (see table 3.1). This implies that the GVB starter will get a lot hotter than the JE starter and this might be a limiting factor for the GVB starter.
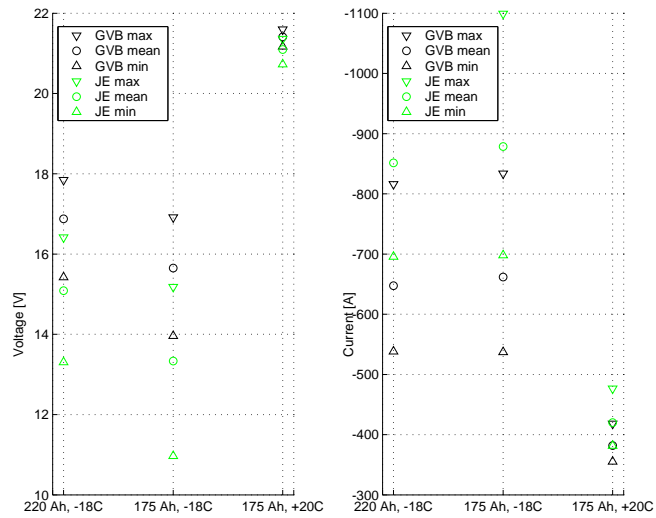
(a) Voltage over starter

(b) Current drawn by starter
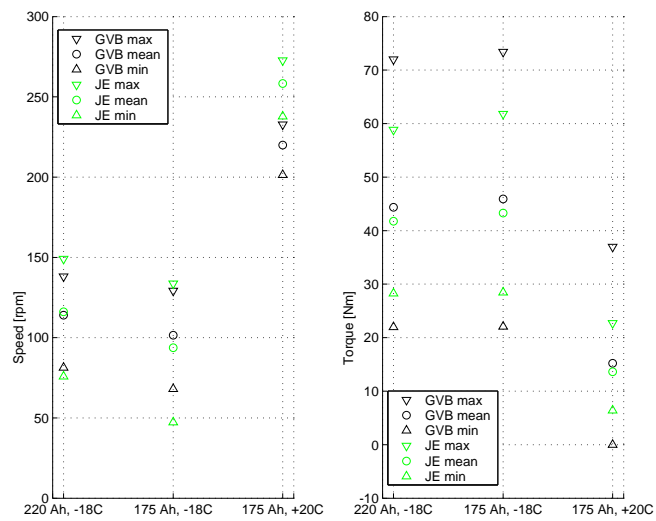
(c) Cranking speed of combustion engine

(d) Torque produced by starter

Figure 6.1: Batteries and temperature varied in simulations of a six cylinder combustion engine.
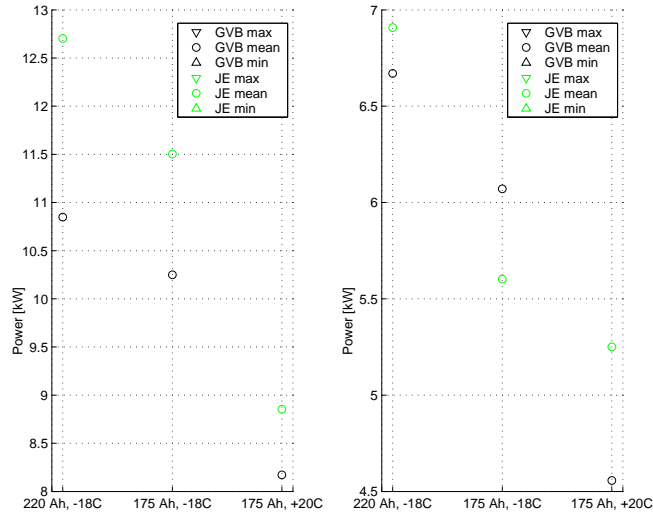
(a) Electric power

(b) Mechanic power
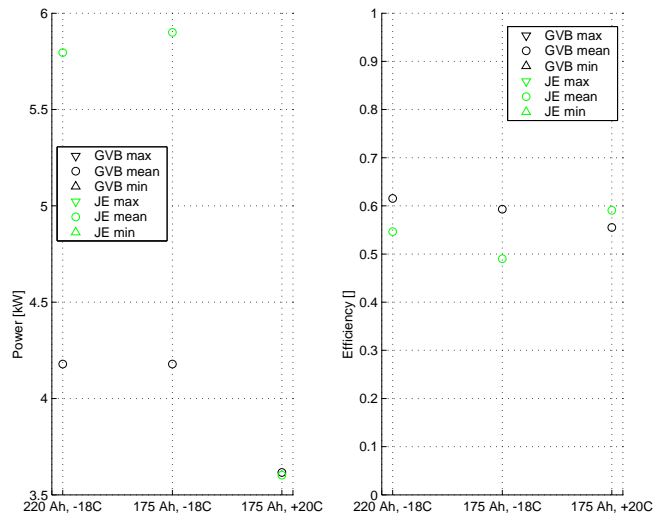
(c) Lost power (heat)

(d) Power efficiency in starter

Figure 6.2: Batteries and temperature varied in simulations of a six cylinder combustion engine, power figures.

6.2   5, 6 and 8 cylinder combustion engines

In this section three different combustion engines are used in simulations. Six, five and eight cylinder engines are simulated at -18°C with 220 Ah batteries. Both the GVB and the JE starter are used. The five and six cylinder combustion engines are models of inline engines. The eight cylinder engine is a model of a V engine. This has the implication that the friction of the eight cylinder engine is just 13% more than the six cylinder engine, not 33% (see chapter 4.5). In the figure 6.3 and 6.4 the results are presented.

Some interesting things to note in these figures:

- More cylinders and higher friction draw more current and give lower cranking speed and thereby lower the voltage and use more battery capacity.

- The five cylinder engine has surprisingly small variations. This is explained by the greater inertia of the five cylinder engine compared to the six cylinder engine.

- The eight cylinder engine has smaller variations.

- The needed power to start is increased with the number of cylinders and the starter motors' efficiency falls. So the lost power, released as heat in the starter motor, increases.

(a) Voltage over starter

(b) Current drawn by starter

(c) Cranking speed of combustion engine

(d) Torque produced by starter
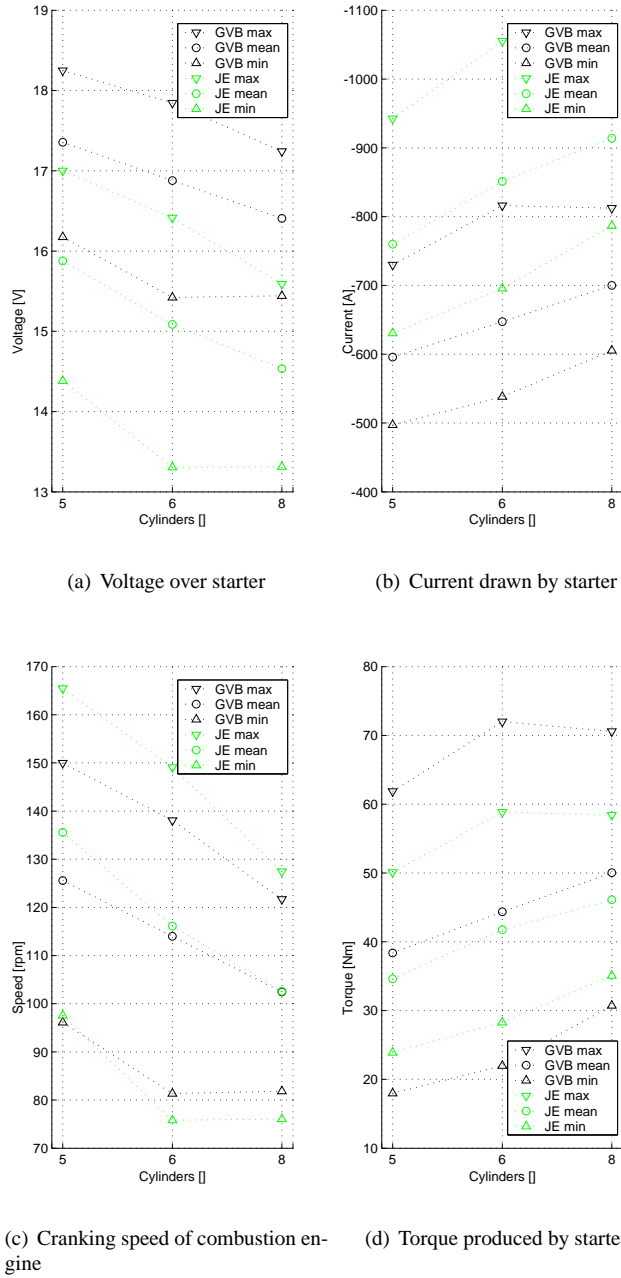
Figure 6.3: Number of combustion engine cylinders varied in simulations of systems with 220 Ah batteries at $-18°$C.
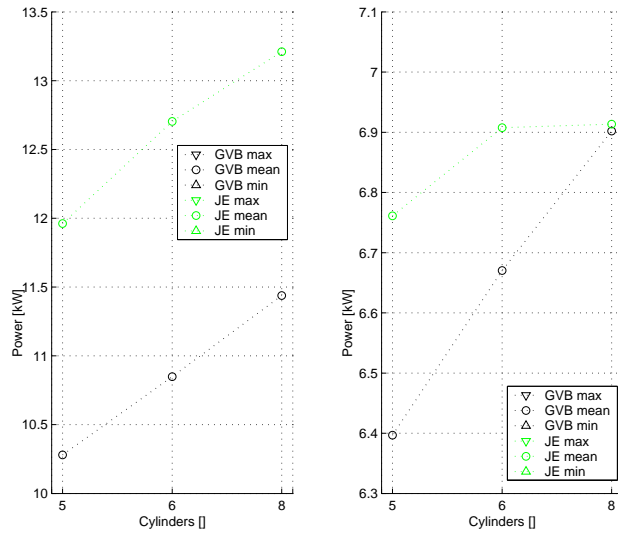
(a) Electric power

(b) Mechanic power
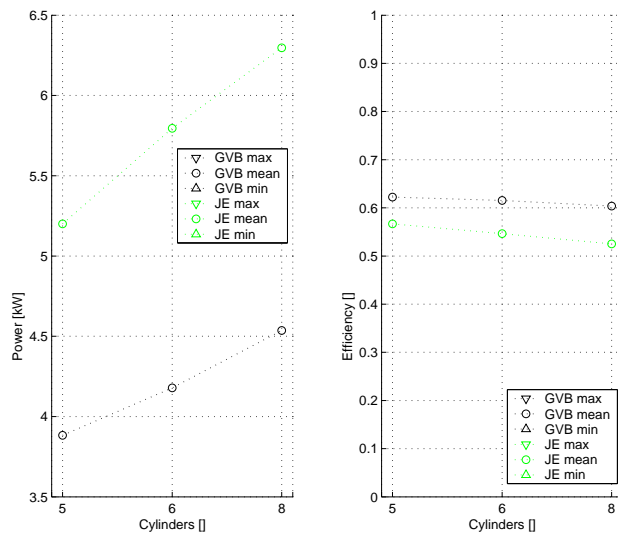
(c) Lost power (heat)

(d) Power efficiency in starter

Figure 6.4: Number of combustion engine cylinders varied in simulations of systems with 220 Ah batteries at $-18°$C, power figures.

6.3   Electric resistance

In this section the effects of increased electric resistance are simulated. A
starting system with a six cylinder engine is simulated with both the JE and
the GVB starter at -18°C. In figure 6.5 and 6.6 the results is plotted for a
system with 175 Ah batteries and in figure 6.7 and 6.8 a system with 220 Ah
batteries.

The increased resistance is modelled in the line resistance, but it could
just as well be modelled as an increased resistance anywhere else in the elec-
tric part of the starting system, like batteries with lower capacity or state of
charge.

The increased resistance has the following effects:

- The voltage falls over the starter, and thereby over the complete elec-
  tric system. If the increased resistance is a greater line resistance the
  system voltage of other components might be higher, but still low due
  to the high current. If the resistance increase is due to lower battery ca-
  pacity or lower state of charge the voltage will drop all over the electric
  system.

- The higher current drawn by the starter increases, but the lower current
  drawn stays at the same value. There is a maximum current the starting
  system can produce, but it is well outside of the models' area.

- The cranking speed of the combustion engine falls.

- The produced torque by the starter has a small increase.

- The lost power, released as heat in the starter motor, is almost constant.

- The efficiency of the starter motors falls. Since the cranking speed of
  the combustion engine also falls, the efficiency of the whole starting
  system falls even further.

(a) Voltage over starter

(b) Current drawn by starter

(c) Cranking speed of combustion engine

(d) Torque produced by starter
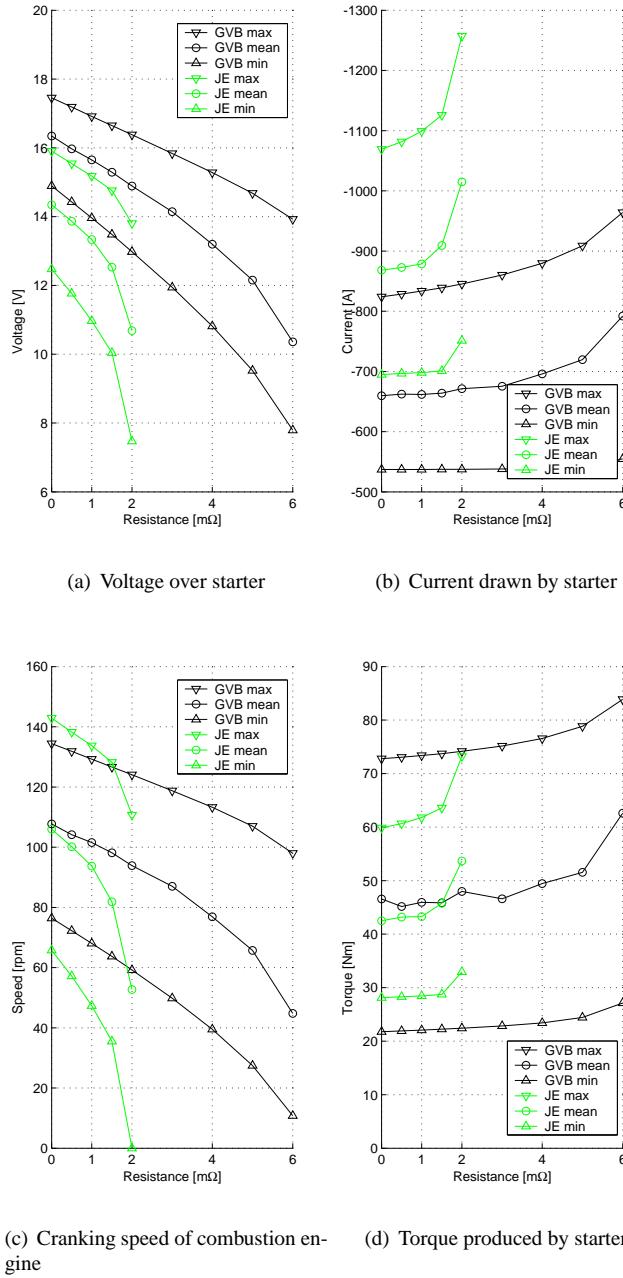
Figure 6.5: Line resistance varied in simulations of a system with 175 Ah batteries and six cylinder engine at $-18°$C.
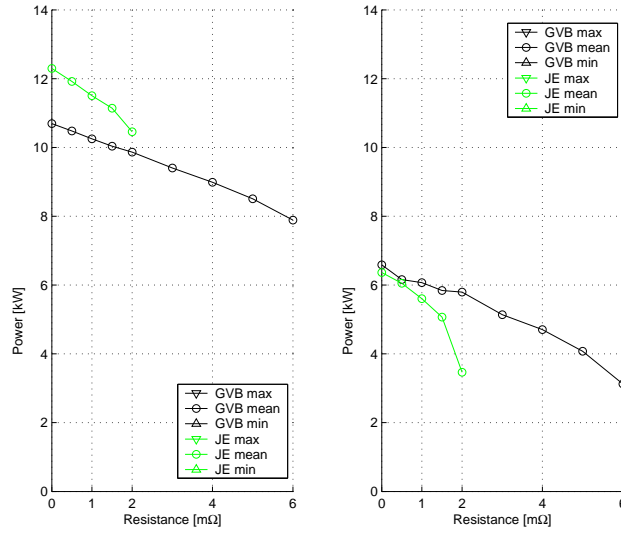
(a) Electric power

(b) Mechanic power
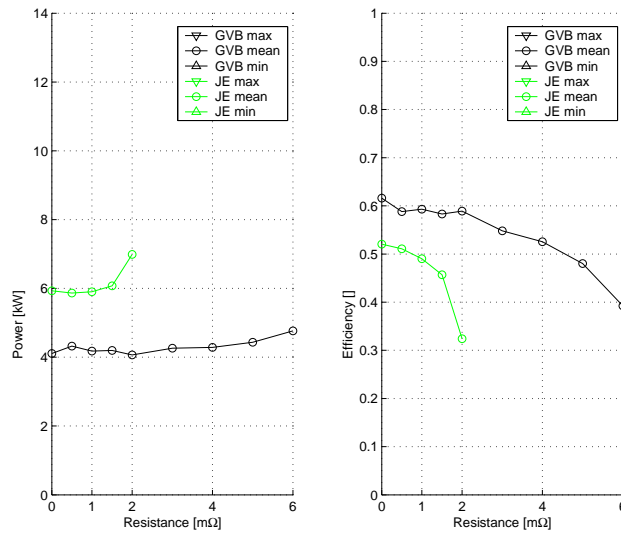
(c) Lost power (heat)

(d) Power efficiency in starter

Figure 6.6: Line resistance varied in simulations of a system with 175 Ah batteries and six cylinder engine at $-18°$C, power figures.
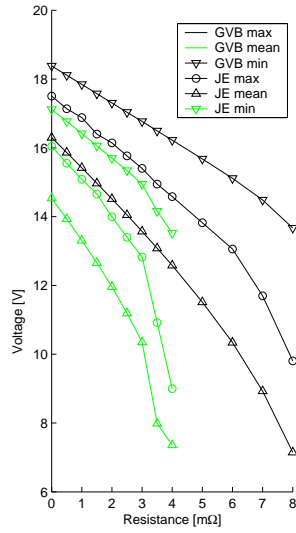
(a) Voltage over starter
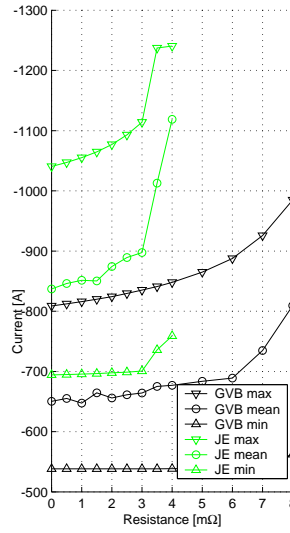
(b) Current drawn by starter
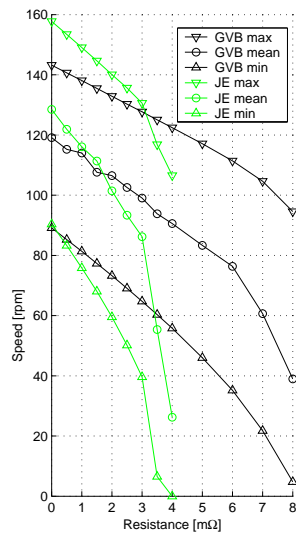
(c) Cranking speed of combustion engine
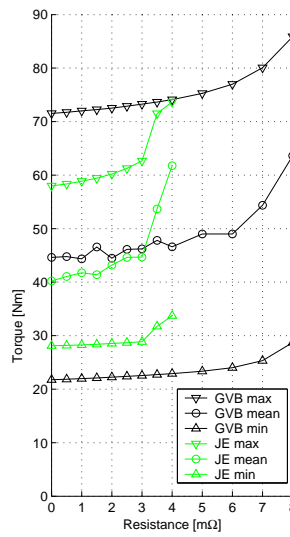
(d) Torque produced by starter

Figure 6.7: Line resistance varied in simulations of a system with 220 Ah batteries and six cylinder engine at $-18°$C.
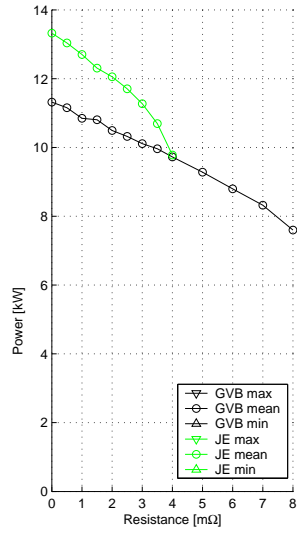
(a) Electric power
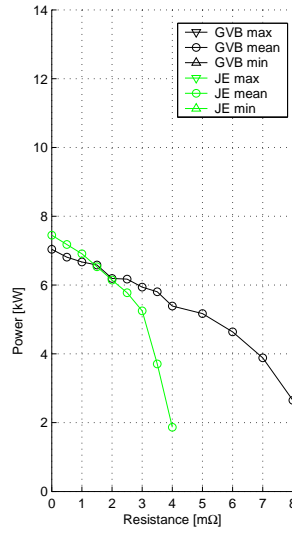
(b) Mechanic power
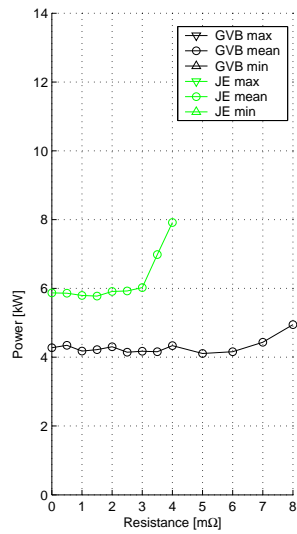
(c) Lost power (heat)
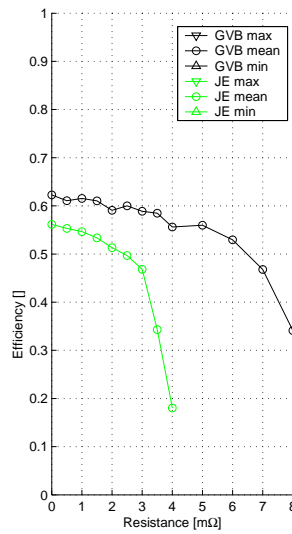
(d) Power efficiency in starter

Figure 6.8: Line resistance varied in simulations of a system with 220 Ah batteries and six cylinder engine at $-18°$C, power figures.

6.4   Starter motor to crank shaft ratio

In this section the effect of the ratio from the starter motor to the crank shaft is investigated. A starting system with 175 Ah batteries and a six cylinder engine is simulated with both the JE and the GVB starter at $-18°$C. The number of teeth on the ring gear has been varied and the results are plotted in figure 6.9 and 6.10. The ratio can be placed at different places in the system, for example in the planetary gear of the starter motor.

Some interesting things to note in these figures:

- Increased number of teeth, and thereby increased ratio, has the following effects; the voltage over the starter increases, the current drawn by the starter decreases, the torque produced by the starter decreases.

- The speed has an optimal ratio value. For the JE starter the value is around 230 teeth and for the GVB around 160. The ring gear has in reality 158 teeth and the GVB starter is much better optimized than the JE starter. This is because the GVB has a possibility to be optimized due to the planetary gear.

- The power efficiency is almost constant.
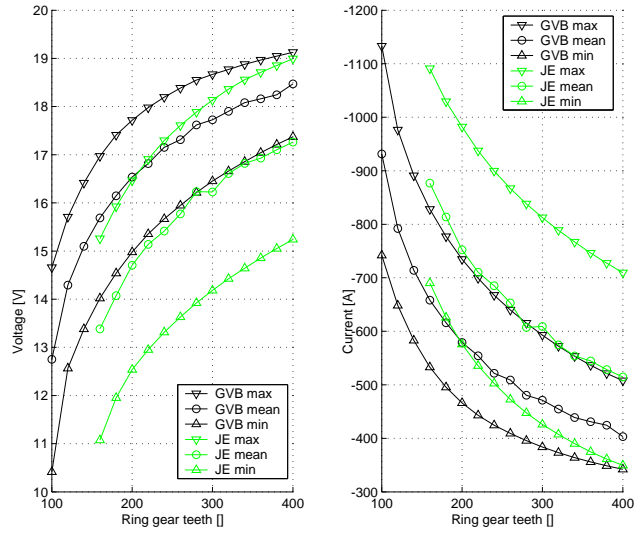
(a) Voltage over starter

(b) Current drawn by starter
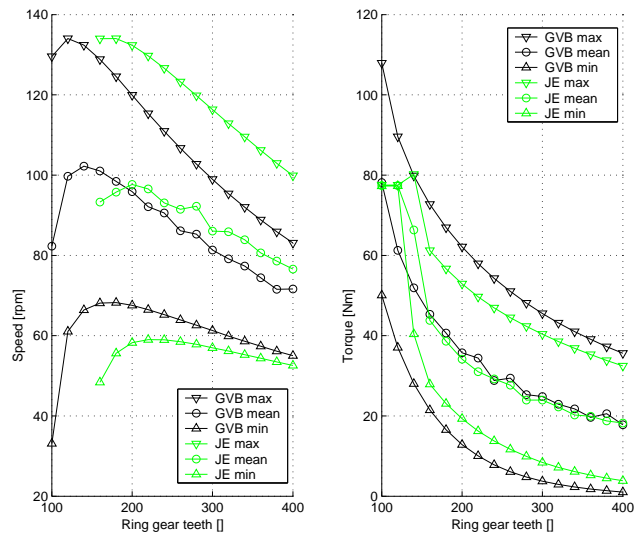
(c) Cranking speed of combustion engine

(d) Torque produced by starter

Figure 6.9: Number of teeth on the ring gear varied in simulations of a system with 175 Ah batteries and six cylinder engine at $-18°$C.

(a) Electric power

(b) Mechanic power

(c) Lost power (heat)

(d) Power efficiency in starter
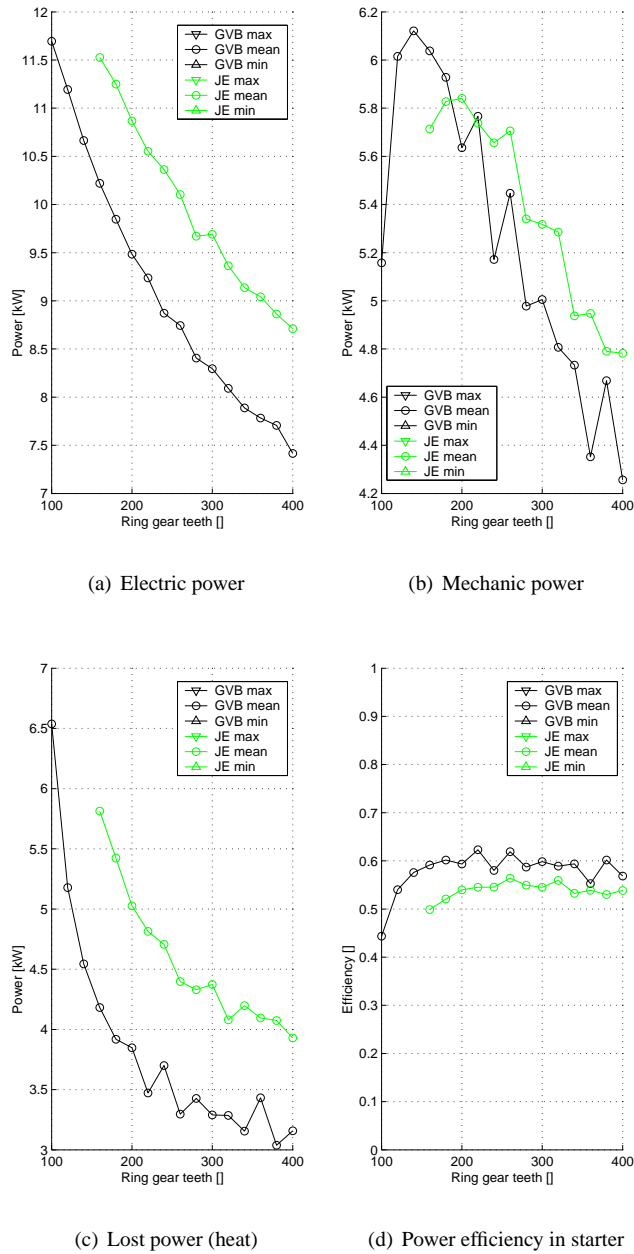
Figure 6.10: Number of teeth on the ring gear varied in simulations of a system with 175 Ah batteries and six cylinder engine at $-18°$C, power figures.

References

[1] Scania CV AB. *Technical regulation TB 1623*. Scania CV AB, Södertälje, Sweden, 2001.

[2] S. Kromlids V. K. Ramachandaramurthy M. Barnes N. Jenkins C.-J Zhan, X. G. Wu and A. J. Ruddell. Two electrical models of the lead-acid battery used in a dynamic voltage restorer. In *IEE Proceedings-Generation, Transmission and Distribution*, volume 150, pages 175–182. IEE, UK, March 2003.

[3] P. Caselitz and R. Juchem. Computer aided design of battery management systems for automobiles – a model for lead acid batteries. Technical Report 980309, Society of Automotive Engineers, Inc., Warrendale, U.S.A., 1998.

[4] M.C. Sultan D.-L. Tang and M.-F. Chang. A dynamic engine starting model for computer-aided control systems design. volume 13, pages 203–222. American Society of Mechanical Engineers, 1989.

[5] Timothy P. Gardner and Naeim A. Henein. Diesel starting: A mathematical model. Technical Report 880426, Society of Automotive Engineers, Inc., Warrendale, U.S.A., 1988.

[6] Robert Bosch GmbH. Technische kundenunterlage – schubtriebstarter je 24 v 6.7 kw. Technical Report Y 001 TU JE 03, K9/SBS6, Germany, 1994.

[7] Robert Bosch GmbH. Basic specification – starter gvb 24 v 6.0 kw. Technical Report Y 001SP3500e, K9/PES, Germany, 1999.

[8] Robert Bosch GmbH. *Starting systems*. Addison-Wesley series in electrical engineering. Robert Bosch GmbH, Stuttgart, Germany, 4 edition, February 1999.

[9] H. Gu. Mathematical modeling in lead-acid battery development. In *Battery Conference on Applications and Advances, 1991. Proceedings of the Sixth Annual*, pages 47–56, 1991.

[10] Günter F. Hohenberg. Advanced approaches for heat transfer calculations. Technical Report 790825, Society of Automotive Engineers, Inc., Warrendale, U.S.A., 1979.

[11] Lubomyr O. Hewko Hsu-Chiang Miao and David A. Fulton. Dynamic modeling and simulation of an automotive engine cranking system. Technical Report 920292, Society of Automotive Engineers, Inc., Warrendale, U.S.A., 1992.

[12] K. F. Hutcheon and R. L. Marks. Developments in starter motor applications to diesel engines. volume 184, pages 97–102. Institution of Mechanical Engineers, 1969-70. Pt. 3A.

[13] Kun-Sik Bae Jung-Kyu Park and Cheon You. Dynamic modelling and simulation of diesel engine starting process. Technical Report 1999-08-0382, Society of Automotive Engineers, Inc., Warrendale, U.S.A., 1999.

[14] Donald J. Pattersson Mark Poublon and Michael Boerma. Instantaneous crank speed variations as related to engine starting. Technical Report 850482, Society of Automotive Engineers, Inc., Warrendale, U.S.A., 1985.

[15] John R. Miller and Susannah M. Butler. Diesel engine starting using battery-capacitor combinations. Technical Report 2001-01-2714, Society of Automotive Engineers, Inc., Warrendale, U.S.A., 2001.

[16] Dah-Lain Tang Myrna Cotran Sultan and Man-Feng Chang. An engine and starting system computer simulation. Technical Report 900779, Society of Automotive Engineers, Inc., Warrendale, U.S.A., 1990.

[17] Atul B. Patil and Nitin S. Ranade. Computer simulation of an i.c. engine during cranking by a starter motor. Technical Report 930626, Society of Automotive Engineers, Inc., Warrendale, U.S.A., 1993.

[18] Philip Reasbeck and James G. Smith. *Batteries for Automotive Use*. Research Studies Press Ltd., Somerset, England, 1997.

[19] C. M. Shepherd. Design of primary and secondary cells ii. an equation describing battery discharge. In *Journal of the Electrochemical Society*, volume 112, pages 657–664, July 1965.

[20] Gordon R. Slemon. *Electic Machines and Drives*. Addison-Wesley series in electrical engineering. Addison-Wesley, United States of America, 1992.

[21] Eckhard Karden Stephan Buller, Marc Thele and Rik W. De Doncker. Impedance-based non-linear dynamic battery modelling for automotive applications. In *Journal of Power Sources*, volume 113, pages 422–430, 2003.

[22] Richard Stone. *Introduction to Internal Combustion Engines*. Society of Automotive Engineers, Inc., Warrendale, U.S.A., 2 edition, 1993.

[23] the International Orgnization for Standardization. *Road vehicles – Electric performance of starter motors – Test methods and general requirements*. Number ISO 8856:1995(E). ISO, Genève, Switzerland, 2 edition, 1995.

Appendix A

Tests

A.1 Tests in engine cell K2

A number of tests were performed at engine cell K2, STC. The tests involved systems of battery, starter and combustion engine or only the engine and cell equipment.

The measuring equipment installed in K2 has an upper sample limit of 10 Hz. This was far too low for the tests to be performed. Therefore a decision was made to use a RoadRunner Mobile 1 for data collection with a TXBAD8-kort. The RoadRunner collected data at 25 kHz and was also used for limited data analysis (down sampling, filtering and analysis during tests). More information about the RoadRunner with accessories can be found at Scania intranet `\\Guran\UserMApp\LMS\Roadrunner_manualer\-Manual_Mobile1_hardware.pdf`. During all tests the pressure in the sixth cylinder was measured with a Kistler Piezoresistive Amplifier Type 4618AD, with pressure sensor 4073A50. More information about the Kistler equipment can be found on the internet at `www.kistler.com`. The rotational speed of the engine was measured in two different ways. An inductive sensor mounted on the crank house at the ring gear of the flywheel sends out 158 pulses per turn of the combustion engine. An optical equipment (AVL Pulse Multiplier 3501-Z031 with sensor AVL Optical Crank Angle Marker 360C_600) senses holes in a disc mounted facing the flywheel. The disc had six hundred holes in one turn of the combustion engine. Unfortunately a multiplier is integrated in the controlling device for the sensor and the signal that is measured has eighteen hundred pulses per combustion engine turn. When the engine turns fast the signal frequency gets close to the maximum measured frequency of the RoadRunner. The signal analysis was able to handle this, but the signal gets more disturbed. A suggested solution is to use other devices to measure crank angle or to modify the AVL pulse multiplier.

The inductive sensor gives very different voltage outputs (high at high

speed and low at low speed). This introduces overhearing to other channels at high voltage and limits the measurement at a too low voltage. If a frequency to voltage device is used a delay is introduced. A suggested solution is to make sure the crank angle measurement is reliable and to remove measure of the inductive sensor.

Both ways to measure speed have no direction, so when the engine stops it is not possibly to tell if the engine started to turn backwards due to a compression from the test results.

The same combustion engine was used during all the tests, a DT1202. The engine is an inline six cylinder equipped according to Scania technical regulation for starter motors [1]. Notable is that no fuel was connected to the engine during all the tests. The fuel was removed to protect the pressure sensor. The Kistler 4073A50 sensor is constructed for up to fifty bars; combustion would very likely destroy the sensor. The sensor is piezoresistive and therefore has a signal which corresponds to the measured pressure. Many other pressure sensors only give a signal when the pressure changes, this works fine for measures with high frequency, but the cranking process is slower than the intended speed. For a good model of the combustion chamber, including combustion, tests have to be performed with a sensor that can both measure the low pressure during cranking and the high pressure when the combustion engine starts to ignite. Alternatively two sensors can be used, but the low pressure sensor must although withstand the combustion without high risk of damage.

A.1.1   Transient torque test

The transient torque pulled by a starter mounted on the combustion engine was measured. For this test a modified EVB-starter was built. The starter's pinion was locked at end position and the shaft that was freed had bridge torsion sensors glued on. The modified starter was calibrated at standstill with weights. The measurement was disturbed by the magnetic field from the starter motor. Current was induced in the sensors and connections to the bridge amplifier. The disturbance was not possible to remove from the measured data. The measured data was not possible to use. A suggested solution is to screen the sensors and connections from the magnetic field.

A.1.2   Starting system tests

Several combinations of full starting system tests were performed. On the combustion engine the three types of starters were mounted. The starters were cranked for twenty seconds, both at $+20^{\circ}$C and -18°C. Each test was repeated three times. At $+20^{\circ}$C the EVB used 175 Ah batteries, all the other tests were performed with 220 Ah batteries. The number of batteries available for the tests was limited. As a result most tests were performed with not completely fully charged batteries. When the test equipment were installed in

the cell and tried out there were several problems with the TXBAD8 card. The card has differential gates but the ground potential differences must be lower than 15 V. Initially the current was measured with shunts, both total current and current drawn by the starter solenoid. The solenoid current must have a ground potential of approximately 25 V over the starter voltage measure. The potential of the shunt was lowered with batteries, but leak current made it impossible to use this method. The solution was to not measure solenoid current. Several different shunts were tried for total current measure, but unreasonable results were found. Probably because limits in the TXBAD8 card. The solution was to measure total current with a Fluke i1010 AC/DC Current Clamp. A suggested solution to the problems with the TXBAD8 card is to connect isolating amplifiers between the card and sensors (today there are no isolating amplifiers availably at STC). The Fluke i1010 is specified for maximum 1000 A, and STC has no equipment for calibrating the Fluke i1010 at higher values. As a result the measured data above 1000 A is probably lower then reality due to the characteristics of a Hall-effect clamp-on probe. A suggested solution is to use a shunt for total current measurement. The connection terminals to the batteries of the starter cables in K2 are of bad quality. A suggested solution is to make new starter cables.

Another suggestion is to also record pressure and temperature on inlet and exhaust gases. This could prove valuable for improvement of the combustion chamber model.

A.1.3   Engine friction test

Torque to rotate the combustion engine was measured from 10 rpm to 300 rpm. The torque was produced by a big electric engine installed in the cell. The electric engine is called brake since it is mostly used as a load to a running combustion engine tested in the cell. Due to the torque measuring equipment installed in the engine cell it was not possible to measure friction versus crank angle. The equipment is highly average building, since the measuring is based on the torsion of the entire electric motor.

The torque was measured with and without compression (injectors removed), at both $+20°C$ and $-18°C$. Due to risk of damaging the engine and time limits, each test was only carried out once. When torque with compression was measured the torque was highly varying. At low speed the torque was highly dependent on crank angle and at around 240 rpm oscillating resonance was found between the engine and the cell equipment. Test results can be viewed in figure A.1.

The tests were performed in the following order: warm environment with compression, warm environment without compression, cold environment without compression, cold environment with compression. During the tests without compression oil leaked down into the cylinder. This oil greased the cylinder and sealed the combustion chamber. The effects are visibly in the test results. It is unlikely that the offset between friction with and without com-
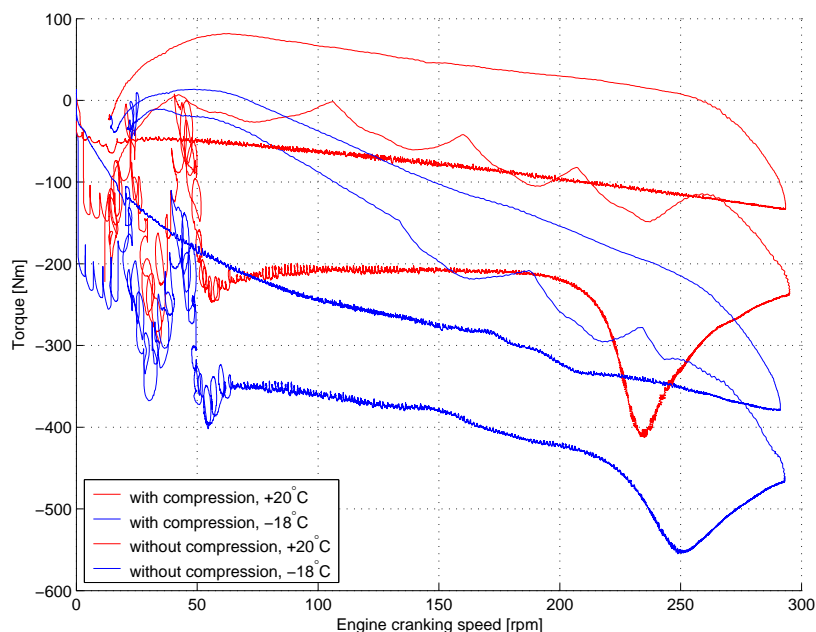
Figure A.1: Measured torque to crank a DT1202 engine in engine cell K2. Cranking is performed from standstill to 300 rpm in three minutes and back to standstill.

pression is lower in a cold environment. Particularly since the pressure was higher in the cold environment, probably due to oil sealing the combustion chamber.

When the system tests were repeated as simulations it was found that the loss of energy in the combustion engine was underestimated. The solution was to increase the friction. As a result the torque measurements of the engine are only used as base for the speed variation of the combustion engine's friction. The decision to model the energy loss as increased friction is based on the problems with the brake's torque measure. The torque measure is constructed to measure the load the combustion engine pulls at high effect. The low speed and other aspects of the test and cell equipment have to be investigated before a new test is done. One solution is to use the equipment used in some of the other cells, a torque meter mounted on the shaft between the combustion engine and brake.

A.1.4   Blow by test

The blow by was measured in the sixth cylinder at standstill. The engine was turned so the all valves and the injector were closed. Then pressured air was

applied to the cylinder. The drop of pressure was recorded when the applied pressure was removed. The results are available in the data from the tests.

A.2   Starter motor tests

A number of tests were done to examine the starter motors' characteristics.

Torque produced by starter motors cannot be measured with the equipment available at STC. The equipment must be calibrated with unavailable equipment or new test equipment must be built or bought.

The resistance of the starter motors cannot be measured at standstill due to too great dependence on armature angle.

The current drawn by the solenoid was measured for a GVB solenoid removed from the GVB starter motor. The results matched the data for the GVB starter.

Copyright

Svenska

Detta dokument hålls tillgängligt på Internet - eller dess framtida ersättare - under en längre tid från publiceringsdatum under förutsättning att inga extraordinära omständigheter uppstår.

Tillgång till dokumentet innebär tillstånd för var och en att läsa, ladda ner, skriva ut enstaka kopior för enskilt bruk och att använda det oförändrat för ickekommersiell forskning och för undervisning. Överföring av upphovsrätten vid en senare tidpunkt kan inte upphäva detta tillstånd. All annan användning av dokumentet kräver upphovsmannens medgivande. För att garantera äktheten, säkerheten och tillgängligheten finns det lösningar av teknisk och administrativ art.

Upphovsmannens ideella rätt innefattar rätt att bli nämnd som upphovsman i den omfattning som god sed kräver vid användning av dokumentet på ovan beskrivna sätt samt skydd mot att dokumentet ändras eller presenteras i sådan form eller i sådant sammanhang som är kränkande för upphovsmannens litterära eller konstnärliga anseende eller egenart.

För ytterligare information om Linköping University Electronic Press se förlagets hemsida: `http://www.ep.liu.se/`

English

The publishers will keep this document online on the Internet - or its possible replacement - for a considerable time from the date of publication barring exceptional circumstances.

The online availability of the document implies a permanent permission for anyone to read, to download, to print out single copies for your own use and to use it unchanged for any non-commercial research and educational purpose. Subsequent transfers of copyright cannot revoke this permission. All other uses of the document are conditional on the consent of the copyright owner. The publisher has taken technical and administrative measures to assure authenticity, security and accessibility.

According to intellectual property law the author has the right to be mentioned when his/her work is accessed as described above and to be protected against infringement.

For additional information about the Linköping University Electronic Press and its procedures for publication and for assurance of document integrity, please refer to its WWW home page: `http://www.ep.liu.se/`

© Fredrik Mellblom
Linköping, 1st October 2004